ELSEVIER

PII: S0032-3861(97)00101-8

Polymer Vol. 38 No. 22, pp. 5623–5641, 1997

0032-3861/97/$17.00+0.00

Heterophase water-in-oil polymerization of acrylamide by a hybrid inverse-emulsion/inverse-microemulsion process

José Hernández-Barajas and David Hunkeler*
Department of Chemical Engineering, Vanderbilt University, Nashville, TN 37235, USA
(Received 10 September 1996)

Heterophase water-in-oil polymerizations of acrylamide have been conducted in the presence of blends of non-ionic stabilizers at moderate monomer concentrations (20%). The initial monomeric system is located outside the inverse-microemulsion domain, yet close to the inverse-macroemulsion/inverse-microemulsion phase boundary. A turbid, viscous and unstable dispersion is produced at the outset and during the intermediate stages of the polymerization. This evolves to an inviscid and non-settling system at high conversions. Transparent inverse latices can also be produced provided that the polymerizations are conducted semi-adiabatically. Small angle neutron scattering (SANS) studies of the initial monomer and reacting systems have found the latices to be particulate with a particle diameter of 150 nm, independent of conversion. The SANS intensities can be fitted using a polydispese spherical particles model. Therefore, these heterophase water-in-oil polymerization systems seem to follow an inverse-macroemulsion-like mechanism. The 'hybrid inverse-microemulsion/inverse-macroemulsion' polyacrylamides produced herein have a smaller radius of gyration in aqueous media relative to those produced by either solution polymerization or a true inverse-macroemulsion polymerization of the same weight-average molecular weight. This is likely due to a large number of intramolecular interactions, such as hydrogen bonds, which are induced by the collapsed nature of the polymer chains in the inverse-microemulsion droplets. The weight-average molecular weight, the radius of gyration and the particle diameter of the final latex are relatively independent of the polymerizations conditions such as initiator level, hydrophilic-lipophilic balance (HLB), temperature and physical changes occurring during polymerization. From a kinetic point of view, the molecular weights of these systems are controlled by transfer to monomer, while transfer to interfacial emulsifier is the polymerization rate controlling step. A reaction mechanism consisting of a number of elementary reactions has been proposed for these heterophase-water-in-oil polymerizations. Agreement with the experimental data is found to be good at different levels of initiator, HLBs and temperature. Despite the limitations of this heterophase water-in-oil polymerizations (the moderate emulsifier levels, low radius of gyration and its inability to increase the weight-average molecular weight beyond 10^6 daltons), this polymerization process can produce final latices that are transparent and non-settling with small particles (< 150 nm). This allows post-reaction chemical modification, e.g. by the Mannich reaction. © 1997 Elsevier Science Ltd.

(Keywords: acrylamide; inverse-emulsion; inverse-microemulsion)

INTRODUCTION

The production of acrylic water soluble polymers is a multi-billion dollar industry in the USA[1]. Polyacrylamide and its copolymers with anionic and quaternary ammonium monomers comprise the majority of the market, which includes applications in paper making (fines retention), the flocculation of municipal and industrial waste water and mining applications. The polymers are generally characterized with molecular weights of the order of 10^7 daltons and are efficient in aqueous solid–liquid separations. Concomitant with the high molecular weight are extreme solution viscosities, even at polymer concentrations as low as several percent. This leads to problems in synthesis, particularly in agitation and heat transfer. The control of polymerizations involving acrylamide monomers is exacerbated by the high enthalpy of polymerization ($\Delta H_p = 19.5$ kcal mol^{-1}) and a propensity to form covalent crosslinks at temperatures above approximately 70°C (intermolecular immidization)[2]. Therefore, in order to control the synthesis of high molecular weight polyacrylamide homo- and co-polymers, while maintaining a commercially viable operation (high monomer concentrations), Vanderhoff *et al.*[3] developed a heterophase water-in-oil polymerization process which he termed 'inverse-emulsion'. This involved the dispersion of an aqueous water soluble monomer, in a continuous organic phase. Stabilization was achieved sterically and the initiating species could reside either in the dispersed water phase (in analogy to suspension polymerization) or in the continuous oil phase (as is the case in classical emulsion polymerization). Further refinements to this process over the last four decades have involved the use of both aromatic and paraffinic continuous phases and various non-ionic emulsifier systems.

* To whom correspondence should be addressed. Present address: Institute of Chemical Engineering (IGC-I), Department of Chemistry, Swiss Federal Institute of Technology, CH-1015 Lausanne, Switzerland

The first synthetic flocculants became available in the USA in the late 1960s[4]. Since the approval of synthetic flocculants by the Food and Drug Administration, several American, European and Japanese firms have commercialized inverse-emulsion technology to produce water soluble polymers. The applications of inverse-emulsion polymerization have continued to expand over the past 20 years and the five-year forecasted growth rates in the production and sales of flocculants are over 5% per annum[5].

Until 1990, the focus of this industrial research and development was focused on inverse-macroemulsion polymerization. Academic research was also heavily skewed towards inverse-emulsion and inverse-suspension polymerizations. For example, Vanderhoff *et al.* at Lehigh continued to publish in inverse-emulsion[6], and the 1980s brought interest from Reichert's group in Germany[7–9], Dimonie's group in Romania[10,11], Pichot and co-workers in France[12–15] and Hunkeler and co-workers in Canada[16–18]. Recently, members from all but one of the pioneering groups have written an article which categorizes and distinguishes inverse-emulsions, inverse-suspensions and inverse-microemulsions[19]. The nomenclature suggested in this collaborative effort has been used throughout this paper.

The 1980s research focus also brought a great deal of understanding as to the mechanism of inverse-emulsion polymerization as well as the kinetic and reactor modelling of these homopolymerization and copolymerization processes[16–18,20]. At the same time, Candau and co-workers were developing 'inverse-microemulsion' polymerization[21–25]. Like inverse-emulsion polymerization, this involved the dispersion of a water soluble monomer in aqueous solution in a continuous organic phase. However, by increasing the emulsifier concentration significantly, thermodynamically stable inverse-microemulsions were produced which had smaller particle diameters and were completely transparent. While this initially appeared to be a scientific curiosity, inverse-microemulsion polymerizations have now been commercialized[26–28] and significant volumes of product are being produced annually. Candau's work included colloidal and kinetic characterizations and optimizations of inverse-microemulsion polymerizations of acrylamide and comonomers with the anionic sodium acrylate monomer. Some of her main advances, in addition to a large contribution to the understanding of the science, were in the application of the cohesive energy ratio concept[29], which showed clearly the advantage of paraffinic continuous phases and allowed the optimization of the emulsifier level and HLB of the surfactant blend. By appropriately matching the molar volume and the solubility parameters of the continuous phase with the lipophilic portion of the emulsifier, inverse-microemulsions could be produced at stabilizer levels as low as 11 wt%. Still, this remained much larger than the 2–4 wt% required for the kinetic stabilization of inverse-emulsions. Candau *et al.*[30] also showed that copolymers with more uniform composition could be produced in inverse-microemulsions compared with solution. Indeed, for the case of acrylamide–sodium acrylate, near-ideal copolymerization kinetics were achieved.

It is not the intent of this paper to review either inverse-emulsion or inverse-microemulsion polymerization since current and comprehensive literature is available for this[31–33]. Rather, we will attempt to point out how the science and technology for both inverse-emulsion and inverse-microemulsion polymerization have recently converged and how this may be exploited. Since their respective inventions by Vanderhoff and Candau, inverse-emulsion and inverse-microemulsion polymerizations have shared the common objective of synthesizing high molecular weight homo- and co-polymers with controlled properties (linear chains, uniform charge density distributions). However, both have offered unique advantages and disadvantages. For example, the lower emulsifier level required of inverse-emulsions had led to earlier and more extensive commercialization. These latices are, however, thermodynamically unstable, and oil separation and shelf-life have been major concerns. Furthermore, process improvements which have been implemented to enhance the colloidal stability, such as the addition of co-surfactants, have generally decreased the molecular weight of the resulting product and the end-use efficiency. Inverse-emulsions also need to be inverted prior to application. Both systems involve the use of organic phases which are not recycled. Current research is now aimed at finding aqueous replacements for these solvents.

Generally, polyacrylamide homo- and co-polymers are sold either as dry powders (Europe), which require redissolution, or as inverse-latices (North America), which require inversion in water. Inverse-microemulsion polymerization has, by comparison, offered a cost and price disadvantage associated with the increased level of emulsifier required. However, they have longer shelf-lives and facilitate post-reaction chemical modification (e.g. Mannich reactions proceed easily in latices following inverse-microemulsion polymerization[26–28]). The inverse-microemulsions are also more easily modified than the inverse-macroemulsions; e.g. microemulsion viscosity can easily be reduced by adding additional continuous phase. Furthermore, during inverse-microemulsion polymerizations significant physical changes can occur, in addition to the chemical transformations. These include large increases in viscosity[31–33], changes in conductivity and turbidity[34–38] and changes in particle size with conversion. Inverse-microemulsions also involve a particle nucleation process rather than the monomer-droplet nucleation which dominates the inverse-emulsion/suspension polymerizations. The net result is that inverse-microemulsions are more complex and generally more difficult to understand than inverse-emulsions. Although a direct comparison of polymers synthesized via inverse-emulsion and inverse-microemulsion is impossible, due to the different emulsifier level requirements, experiments in our laboratory have indicated that inverse-emulsions can produce polymers with molecular weights in the 1.5×10^7 dalton range, whereas inverse-microemulsions are limited to approximately 10^7 daltons, when the same surfactant system was used in both cases. The molecular size in solution is also smaller in inverse-microemulsion (radius of gyration, R_g approximately 150 nm) compared to inverse-emulsion polymers ($R_g > 200$ nm). More importantly, inverse-microemulsion latices are small (of the order of 100 nm). This is less than the radius of gyration of the polymer coil and, as Candau *et al.*[39] have pointed out, the polymer chains in an inverse-microemulsion droplet are in a highly collapsed state.

Objectives

The primary purpose of the research outlined in this paper is to understand physically, mechanistically and

kinetically the heterophase water-in-oil polymerizations of acrylamide in the presence of moderate non-ionic emulsifier concentrations. These systems, while transparent and with a long shelf-life at the completion of the reaction, are turbid and susceptible to coagulation and settling at the outset and through much of the intermediate conversion regime. That is, while the final latex is a non-settling and transparent water-in-oil system, it is not formed from a monomer inverse-microemulsion, but rather evolves or is induced from an inverse-macroemulsion. Commercially, the understanding of these systems is important since their formulation utilizes surfactant levels lower than those required for the preparation of a monomer inverse-microemulsion (typically above 10 wt%, and occasionally as high as 30 wt%). However, by probing the changes in the phase diagram during polymerization, the local temperature of inverse-latices (it will be demonstrated later in this paper that some inverse-latices can be much hotter than the continuous phase) and the possibility of inducing transformations from inverse-emulsions to inverse-microemulsions through process changes, we will show that useful polymers can be produced by hybridizing the inverse-emulsion and inverse-microemulsion processes. Specifically, we will use the moderate stabilizer levels which characterize inverse-macroemulsions and evolve a thermodynamically unstable system into a thermodynamically stable inverse-microemulsion. We will also show that this can be done while producing molecular weights in the 10^7 dalton range. Therefore, we are combining the advantages of inverse-emulsion formulations (low emulsifier levels and high polymer molecular weight) with those of inverse-microemulsion (a thermodynamically stable, non-settling product and facile post-reaction chemical modification). We will refer to this polymerization process generically as a 'hybrid heterophase water-in-oil polymerization'. However, it is clear that the product is a transparent latex which has non-settling properties after a period of over one year in the laboratory.

EXPERIMENTAL

Materials and purification

Two grades of acrylamide monomer were used in this investigation. For polymerizations conducted at a HLB of 8.5, solid crystals of acrylamide (Cytec Industries Inc., Charlotte, NC) were used without further purification. Electrophoresis grade acrylamide (Fisher Scientific, Norcross, CA) was also used for a set of isothermal experiments. These were conducted at a HLB of 7.8, which corresponded to an optimum for this particular grade of monomer.

2,2′-Azobis(4-methoxy-2,4-dimethylvaleronitrile) (V70, Wako Chemicals USA, Inc., Richmond, VA) was recrystallized from methanol at −15°C and then dried *in vacuo* at temperatures between −5 and 0°C. It was subsequently stored at −5°C in a freezer.

Certified ACS EDTA (ethylenediamine tetraacetic acid, disodium salt dihydrate, Fisher Scientific, Norcross, GA) was used as a chelating agent in the polymerizations with unpurified monomers.

Isopar-M (Exxon, supplied by ChemCentral, Nashville, TN), an isoparaffinic mixture with a boiling range between 204 and 247°C, was chosen as the continuous phase.

Emulsifiers were supplied in unbleached (peroxide free) form from ICI Americas (Wilmington, DE). These included polyoxyethylene sorbitan trioleate (Tween 85), polyoxyethylene sorbitan hexaoleate (G-1086), sorbitan sesquioleate (Arlacel 83) and sorbitan monooleate (G-946). They were subsequently purified using an extraction and heat treatment method. This involved repeated washing with acetone to remove any soluble sodium oleate (the largest impurity by mass, about 1–3 wt%). The surfactants were then maintained under vacuum at 40°C for 5 days in order to strip any other volatile components and decompose any species which could initiate the reaction.

The organic phase mixture (Isopar-M and surfactants) was filtered using a 0.45 μm Metricel membrane filter (Fisher Scientific, Norcross, GA) prior to polymerization.

The water used was Type I reagent grade water with a resistivity of at least 18 $M\Omega\,cm^{-1}$ obtained through a series of deionization and organic scavenger cartridges (Continental Water Systems Corp., San Antonio, TX).

Blank inverse-microemulsion polymerizations, in the absence of initiator (V70), showed no monomer conversion in polymer, even after 1 h at 40°C, indicating the absence of any radical generating impurities. The presence of peroxides and other impurities that could initiate the free radical polymerization has been a problem which has plagued many other researchers of heterophase water-in-oil polymerizations. This has been the principal reason why kinetic studies have not been reported in inverse-microemulsion polymerization of acrylamide with non-ionic fatty acid ester based emulsifiers. The purification process outlined above has given us confidence that the rate of polymerization which we observe is indeed an intrinsic reaction rate caused by the thermal decomposition of the initiator. In the following section we will demonstrate that the initiator concentration does indeed influence the kinetics.

Polymer synthesis and temperature control

Polymerizations were performed in a 5-l 316-stainless steel reactor equipped with an external heating/cooling jacket. The reactor internals were custom machined and polished to reduce the coagulum build up (coagulum decreases the heat transfer coefficient). Using a digital data acquisition from a platinum RTD and a Macintosh computer running Labview (an object oriented language), the temperature of the reactor was controlled to within ±0.5°C using an error-squared PID (proportional-integral-derivative) algorithm by varying the chilled water-to-steam ratio entering the cooling jacket. If necessary, in addition to the prechilled water/steam feed to the cooling jacket, prechilled ethylene glycol (4°C) could be circulated through an internal cooling coil to increase the cooling capacity. The reactor was sparged continually with purified 99.99% nitrogen (AL Compressed Gas, Nashville, TN) to remove any residual oxygen, which could consume radicals and interfere with the polymerization. The initiator, in solution with Certified ACS acetone (Fisher Scientific, Norcross, GA), was injected through a septum cap placed at the top of the reactor to start the polymerization. Samples were withdrawn periodically at fixed time intervals by means of a bottom flush valve. Further details of the polymerization procedure have been reported elsewhere[40].

An example of the temperature profile of an isothermal inverse-microemulsion polymerization is shown in *Figure 1*. The experimental conditions are reported in *Table 1* (Run ME3). The temperature control is ±0.5°C.

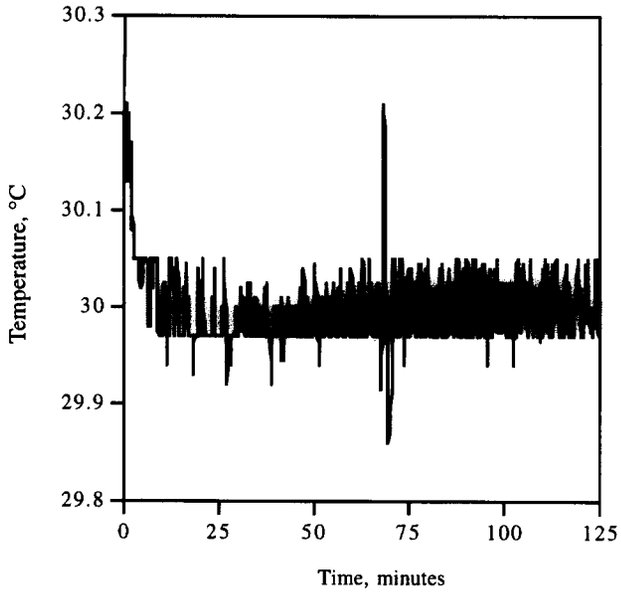

Figure 1 Temperature profile for an inverse-microemulsion polymerization of acrylamide using an error-squared PID controller. Experimental conditions for this polymerization are given in *Table 2* (ME3)

To our knowledge, this represents the first report of an isothermal inverse-microemulsion in the literature. This advance has enabled us to conduct kinetic studies on inverse-microemulsion polymerization using non-ionic surfactants. A kinetic investigation of these systems has been advocated for years by leaders in inverse-microemulsion polymerization, such as Candau. However, the investigations have not been possible due to the emulsifier soluble impurities, which spontaneously initiate the free radical reaction cascade. The results presented herein therefore represent a significant and necessary step in the quantitative understanding of inverse-microemulsion polymerization.

Conversion measurements based on residual monomer concentration

The determination of conversion of acrylamide monomer to polymer was performed using a novel phase inversion high performance liquid chromatography (h.p.l.c.) method with a micellar mobile phase[41]. This procedure begins with the inversion of the inverse-emulsion (water-in-oil) into a direct emulsion (oil-in-water) using Tergitol TMN-10 (Union Carbide Chemcials and Plastics Co., Danbury, CT) as an inverting surfactant and deionized water, under strong agitation. The monomer is then separated from the polymer by size exclusion chromatography using a micellar mobile phase. The h.p.l.c. system consisted of a Rheodyne 7725i injector (Cotati, CA) and a Hitachi 16000 isocratic pump (Hitachi Instruments, Tokyo, Japan). A Shodex OHPAK SB-800P column (JM Science, Buffalo, NY) was used as the stationary phase with 25×10^{-3} M sodium dodecyl sulfate (electrophoresis-grade SDS, Fisher Scientific, Norcross, GA) in highly deionized water as the mobile phase. An ultraviolet (u.v.) detector (Hitachi L-4000H), operating at a wavelength of 214 nm, was used to measure the monomer absorption. The peak heights were used to construct a calibration table and for the analysis of the unknown samples. Chromatograms were collected on either a 286 or a 486 computer running Viscotek GPC PRO Version 4.01 software (Houston, TX).

Figure 2 shows conversion–time plots of replicate polymerizations. The data illustrate that the control of the polymerization, as determined by the rate, is reproducible.

Particle size estimation

The particle size of the final inverse-microemulsions was measured by dynamic light scattering. The procedure involved the dispersion of one drop (nominally 0.0200 g) of an inverse-microemulsion sample in 20 ml of Isopar-K (Exxon, supplied by ChemCentral, Nashville, TN). This was agitated for a period of 2 s and placed immediately in the goniometer (Brookhaven BI-DS). A 2-W argon ion laser (Lexel Laser, Inc., Fremont, CA) operating at a power of 20 mW was used as a radiation source. Data acquisition was carried out for a period of 20–30 s using a 486 PC containing a Brookhaven BI9000 card. Particle diameters were inferred from the Stokes–Einstein relationship from measurements of a mean diffusion coefficient. Various subroutines were also used to estimate the particle size distribution including Non-Negatively Constrained Least Squares (Multi-Pass) and a CONTIN program. Measurements were performed at

Table 1 Experimental conditions for inverse-microemulsion studies using purified acrylamide

Run	G-946 (g)	Tween 85 (g)	Isopar-M (g)	Acrylamide (g)	Water (g)	V-70 (g)	HLB	Temp. (°C)
ME3	57.3	62.7	630	300	450	0.20	7.8	30
ME6	57.3	62.7	630	300	450	0.30	7.8	30
ME7	57.3	62.7	630	300	450	0.30	7.8	30
ME8	57.3	62.7	630	300	450	0.40	7.8	30
ME9	57.3	62.7	630	300	450	0.50	7.8	30
ME11	57.3	62.7	630	300	450	0.75	7.8	30
ME10	53.7	66.3	630	300	450	0.50	8.0	30
ME12	50.2	69.8	630	300	450	0.50	8.2	30
ME13	57.3	63.7	630	300	450	0.50	7.8	35
ME14	57.3	62.7	630	300	450	0.50	7.8	25

Experiments ME6 and 7 were performed to test reproducibility of the kinetic measurements. Experiments ME3, 7, 8, 9 and 11 were carried out to study the effect of initiator on the polymerization rate and the final polymer microemulsion characteristics. Experiments ME9, 10 and 12 were conducted to study the effect of HLB on the polymerization rate and the final polymer microemulsion characteristics. Experiments ME9, 13 and 14 illustrate the effect of temperature on the polymerization rate and final polymer microemulsion characteristics

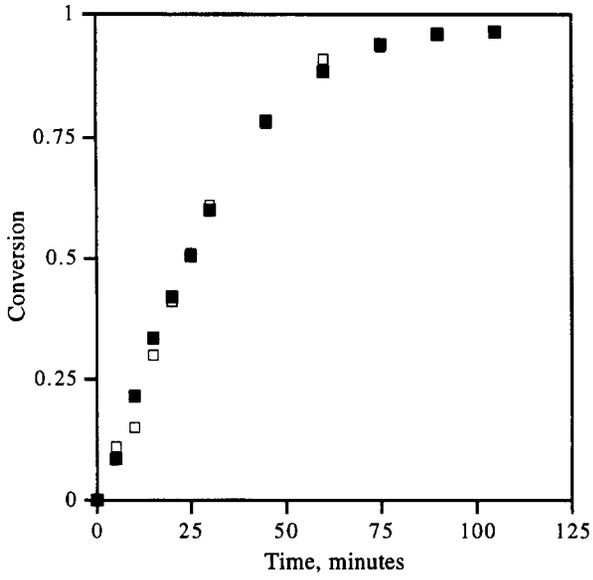

Figure 2 Reproducibility studies for the inverse-microemulsion polymerization of acrylamide using V-70 as initiator with runs ME6 (■) and ME7 (□). Experimental conditions: $T = 30°C$, [M] = 3.29 mol/L_w [I] = 0.972 mmol/L_o, HLB = 7.8, 8 wt% emulsifier, 50/50 wt% aqueous phase/oil phase. Emulsifier system: polyoxyethylene sorbitan trioleate/sorbitan monooleat

25°C with disposable presterilized 20 ml glass stationary cells (Fisher Scientific, Norcross, GA).

Molecular weight determination

Static light scattering experiments were also performed on the Brookhaven system using a laser intensity of 20 mW. Polyacrylamide aliquots were withdrawn from the reactor and precipitated immediately in Certified ACS acetone (Fisher Scientific, Norcross, GA). These were then dried to constant weight under vacuum for 12 h at 25°C. A stock polyacrylamide solution (1000 ppm) was prepared directly in 1.0 M Certified ACS sodium chloride (Fisher Scientific, Norcross, GA). Following complete dissolution (several days), the stock solution (approximately 1 mg ml^{-1}) was filtered twice through 0.65 μm Nucleopore cylindrical pore membranes (Fisher Scientific, Norcross, GA). The stock solution was then diluted with aqueous sodium chloride in a laminar flow hood and placed in 30 ml polypropylene centrifuge tubes (Fisher Scientific, Norcross, GA). These were centrifuged at 21 000 g for 4 h using a Marathon 21 K centrifuge (Fisher Scientific, Norcross, GA). The centrifuge tubes were then returned to the laminar flow hood and the solutions were transferred to precleaned 20 ml scintillation glass vials. Following the sealing of the vials, the samples were analysed within 1 h of being removed from the centrifuge, and in all cases the molecular weight estimates were based on four independent angular scans of each sample. The sodium chloride solvent was recirculated for a period of 24 h through a nylon filter (0.2 μm). This provided a virtually dust free solvent.

Small angle neutron scattering measurements

Small angle neutron scattering (SANS) was used to investigate the structure of our inverse-microemulsions. These studies were conducted on both the initial monomeric and reacting systems prepared immediately prior to SANS experiments. The polymerization was carried out non-isothermally in a 50 ml three-necked round bottom flask using electrophoresis grade acrylamide, deuterium oxide (99.5%, Cambridge Isotope Laboratories, Andover, MA), Isopar-M and mixtures of peroxide-free and purified polyoxyethylene sorbitan hexaoleate (G-1086) and sorbitan sesquioleate (Arlacel 83). The polymerization was initiated with benzoin isobutyl ether (90%, Aldrich, Milwaukee, WI) using a long wave u.v. lamp (Blak-Ray, Model B100 AP, Upland, CA). The peak temperature was controlled by the exposure time to u.v. radiation and by moving the distance from the u.v. lamp to the reactor and never exceeded 55°C. The small reactor was sparged continuously with purified 99.99% nitrogen to remove any residual oxygen for at least 15 min prior to the exposure to u.v. radiation. Samples were withdrawn by means of a 10 ml disposable syringe and received in 20 ml scintillation glass vials containing 0.1 μl of 2 wt% hydroquinone in highly deionized water to stop the reaction. Part of this sample was placed in 1 ml quartz Hellma cells (Hellma, Jamaica, NY) with a 1 mm pathlength and taken immediately to the sample holder of the SANS facility; the rest of the sample was precipitated in certified ACS acetonitrile (Fisher Scientific, Norcross, GA) to measure conversion using a CN column and a method described elsewhere[42].

The SANS measurements were performed on the W.C. Koehler 30 m SANS facility at the Oak Ridge National Laboratory[43]. The neutron wavelength was 4.75 Å ($\Delta\lambda/\lambda \approx 5\%$). The sample–detector distances were 3.2 and 10 m and the data were corrected for instrumental background and detector efficiency on a cell-by-cell basis, prior to radial averaging to give a Q range of $0\,Å^{-1} < Q < 0.25\,Å^{-1}$. The coherent intensities of the sample were obtained by subtracting the intensities of the corresponding blanks, which formed only a minor correction (10%) to the sample data. The net intensities were converted into an absolute (±5%) differential cross-section per unit sample volume (in units of cm^{-1}) by comparison with precalibrated secondary standards, based on the measurement of beam flux, vanadium incoherent cross-section, and the scattering by water and other reference materials[44]. Data were collected for periods ranging from 10 to 30 min. A more detailed description of the experiments will be provided in a subsequent publication.

Experimental conditions

For our kinetic studies, the isothermal inverse-microemulsion polymerizations of acrylamide were carried out over the temperature range 25–35°C. The surfactant and monomer levels were 8 and 20 wt%, respectively. The specific experimental conditions for each polymerization using the unpurified and purified acrylamide are listed in *Tables 1* and *2*, respectively. For the SANS studies, the experimental conditions for each polymerization are listed in *Table 3*.

RESULTS AND DISCUSSION

Non-isothermal polymerizations with unpurified acrylamide

Inverse-microemulsion research has been, thus far, exclusively dedicated to semi-adiabatic processes. These have involved temperature increases during the polymerization as a consequence of the large heat of the

Table 2 Experimental conditions for inverse-microemulsion studies using unpurified acrylamide

Run	G-946 (g)	Tween 85 (g)	Isopar-M (g)	Acrylamide (g)	Water (g)	V-70 (g)	HLB	Temp. (°C)
MEM1	60.0	100.0	840.0	400.0	600.0	0.275	8.5	Non-isothermal
MEM2	60.0	100.0	840.0	400.0	600.0	0.275	8.5	Non-isothermal
MEM3	60.0	100.0	840.0	400.0	600.0	0.275	8.5	30

0.25 g of EDTA were used; MEM1 had a peak temperature of 72°C; MEM2 had a peak temperature of 54°C

Table 3 Experimental conditions for inverse-microemulsions used in the SANS studies

Experiment number	G-1086 (g)	Arlacel 83 (g)	Isopar-M (g)	Acrylamide (g)	D20 (g)	HLB
3	0.8711	0.3782	6.2261	4.5054	3.0150	8.3
6	0.7549	0.4374	6.3308	2.999	4.5139	7.8
9	2.3992	1.6017	19.9185	10.0005	14.9998	7.6
10	4.7891	3.2025	44.3223	15.0188	3.6086	7.6

The initial systems are located outside the inverse-microemulsion domain; 150–200 ppm of benzoin isobutyl ether based on acrylamide were used to initiate the polymerizations in the presence of u.v. illumination

reaction. These non-isothermalities have been as low as 2–3°C for the kintic studies in small 100 ml beakers[39] and as high as 30°C for commercial batch reactors[26–28]. In a subsequent part of this paper we will show, through an analytical model, that local overheating can occur in inverse-microemulsion droplets due to the very large macroradical concentrations, which cause extreme heat generation rates per unit volume. This phenomenon is exacerbated by high internal viscosities which result in low heat transfer efficiencies (the heat transfer coefficient is a decreasing function of particle size). This 'problem' of local overheating may be acute since it can account for temperature differences between the particle and the continuous phase as high as 30°C. Given that these non-isothermal polymerizations reach 55–60°C at high conversions it is quite possible that the internal temperature of the droplets may reach >80°C. This is potentially a disadvantage of inverse-microemulsion polymerization since polyacrylamides are known to branch at temperatures above approximately 70–75°C (intermolecular immidization)[2].

Changes in physical parameters throughout the polymerization

Figure 3 shows the changes in viscosity and turbidity measured during a non-isothermal polymerization of unpurified acrylamide. As the conversion of monomer-to-polymer proceeds, the viscosity of the system rises. Indeed, *Figure 3* can be said to represent a fingerprint of these inverse-microemulsion polymerizations, the understanding of which has motivated further research. Historically, the increase in viscosity has been explained, in the case of bicontinuous or monomeric highly swollen lamellar inverse-microemulsions, to be due to the formation of very large macromolecules in the semi-continuous aqueous domains, which are insoluble in the oily domains. The subsequent decrease in viscosity is due to the formation of a particulate inverse-microemulsion which corresponds

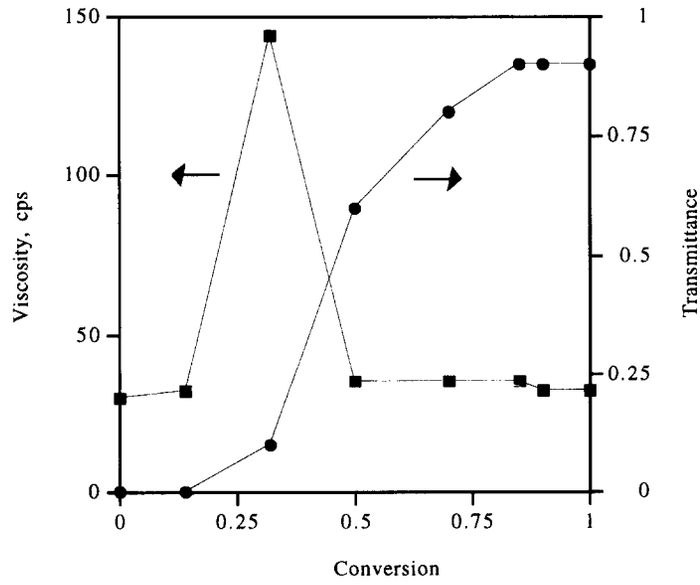

Figure 3 Shear viscosity (■) and turbidity (●) as a function of conversion for a non-isothermal inverse-microemulsion polymerization of acrylamide using V-70 as initiator. Experimental conditions: $T = 30°C$, $[M] = 3.29\,mol/L_w$, $[I] = 0.972\,mol/L_o$, HLB = 8.5, 8 wt% emulsifier, 50/50 wt% aqueous phase/oil phase. Emulsifier system: polyoxyethylene sorbitan trioleate/sorbitan monooleate

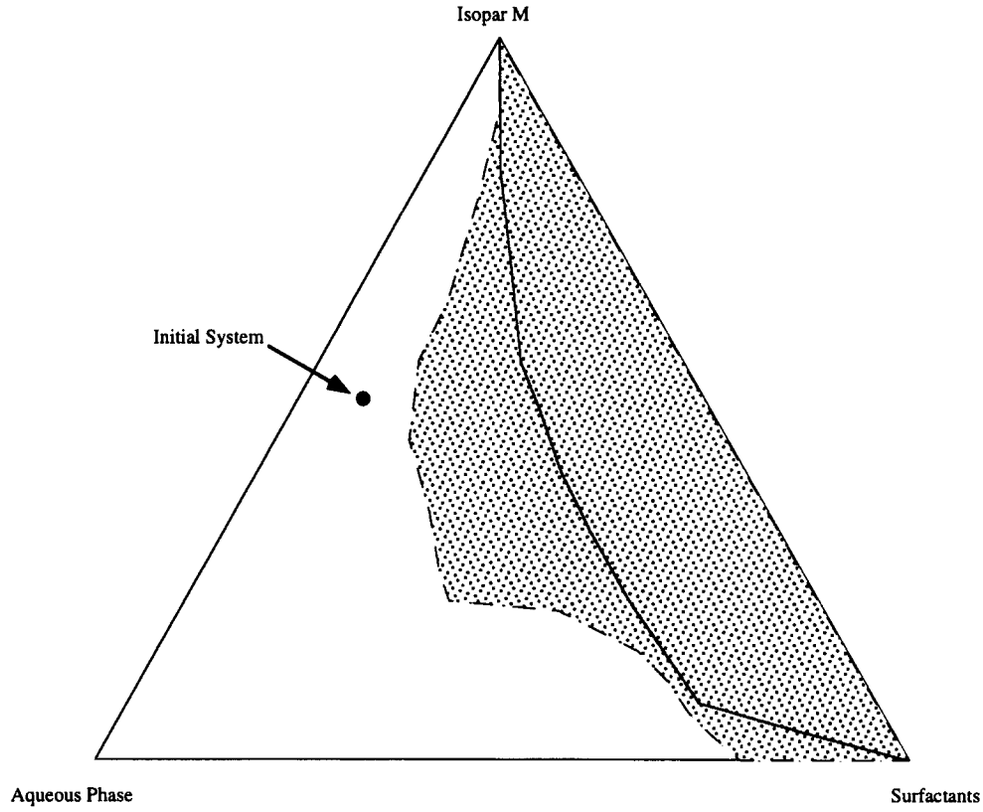

Figure 4 Phase diagram for the acrylamide/water (40 wt%)/Isopar-M/surfactants: polyoxyethylene sorbitan hexaoleate/sorbitan sesquiolate (—) or polyoxyethylene sorbitan trioleate/sorbitan monooleate (– –) at 22°C and HLB = 8.5. The microemulsion domain is the shaded region

to the elimination of the semi-continuous aqueous phase[45]. However, our system was not bicontinuous at any stage of the polymerization and we were unable to detect pure liquid crystal domains with the polyoxyethylene sorbitan trioleate/sorbitan monooleate system at any emulsifier concentration at a HLB of 8.5. Pure liquid crystal structures were, however, observed in the polyoxyethylene sorbitan hexaoleate/sorbitan sesquiolate system at the same HLB at emulsifier levels of approximately 50 wt% using small angle X-ray diffraction. This is certainly well beyond the concentrations of emulsifier utilized in our polymerizations (8%) and cannot account for the viscosity behaviour.

Figure 4 shows a phase diagram for the acrylamide/water (40 wt%)/Isopar-M/surfactants system at 22°C used in our polymerizations. Clearly, the monomeric formulation is quite close to the phase boundary. This inverse-microemulsion/inverse-macroemulsion phase boundary is dependent on the level of monomer, polymer concentration and temperature (*Figure 5*). Given this, we offer the following explanation for the sudden changes in viscosity and turbidity observed as a function of conversion (*Figure 3*). At low conversions, a polymer is produced which is partially located in the continuous phase. This has been confirmed through rheological measurements which have identified low conversion samples to be non-Newtonian pseudoplastics. As the conversion increases the consumption of interfacial monomer causes the interfacial tension to rise. This is offset by an increase in the internal droplet temperature, which lowers the interfacial tension. The net effect is that the inverse-microemulsion domain shifts outwards (enlarges). This engulfs our initial point on the phase diagram and an inverse-microemulsion system is produced at a conversion of less than 10%. This transition is accompanied by a sudden decrease in viscosity and a reduction in turbidity, as would be expected. Immediately following the transition from a turbid viscous system to a clear inviscid inverse-microemulsion the heat generation begins to increase rapidly.

The degree of purity of the acrylamide monomer influences the optimal HLB for conducting inverse-microemulsion polymerizations. This optimum is defined based on the transparency of the final inverse-microemulsion as well as the viscosity rise during the intermediate phase transformation period. We have observed that if the viscosity rise is sufficiently large, or occurs at too high a conversion, e.g. above 50%, then the system is unable to transform itself into an inverse-microemulsion. Given that the transition from a turbid viscous system to an inviscid transparent inverse-microemulsion is accompanied by massive increase in the heat generation rate, it appears that this transition must occur at sufficiently low conversions so that enough monomer remains unreacted to generate heat upon polymerization, which increases the temperature and permits a shift in the phase boundary. Lowering the initial HLB has the effect of reducing the magnitude of the viscosity increase and lowering the rate by permitting greater heat transfer and limiting the influence of diffusion on the termination and transfer reactions. The fact that higher purity acrylamide requires a lower HLB indicates that there is an optimum reaction rate for inverse-microemulsion polymerizations. Moderate reaction rates correspond to low levels of coagulum formation and also facile reactor cleanup. At low rates of reaction, the heat generated following the macro-to-microemulsion transition is insufficient to move the phase boundary (the temperature rise is small and the lowering of the interfacial tension is insufficient) and one cannot induce the formation of an inverse-microemulsion, at least not without a post-reaction heat treatment.

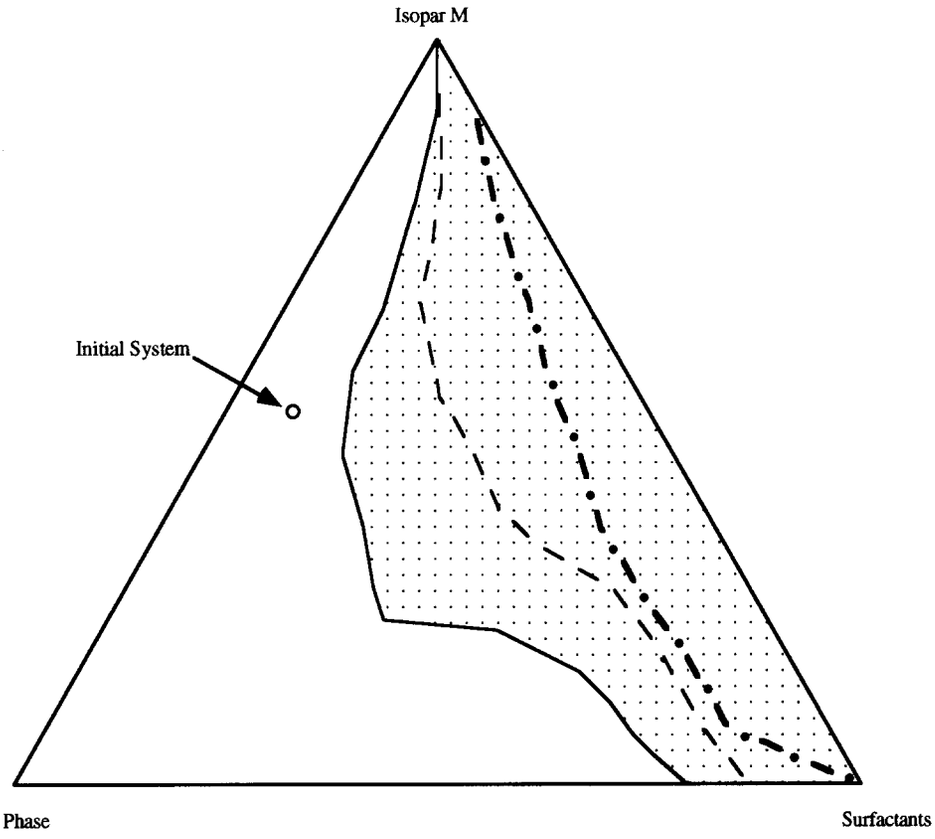

Figure 5 Phase diagram for the acrylamide/water (40 wt%)/Isopar-M/surfactant (—), acrylamide/water/(40 wt%)/100 ppm of polyacrylamide of high molecular weight/Isopar-M/ surfactant (- -), water/Isopar-M/surfactant (- · -). Surfactants: polyoxyethylene sorbitan trioleate/sorbitan monooleate at 22°C and HLB = 8.5. The microemulsion domain is the shaded region

The inverse-latices produced by non-isothermal polymerizations are almost completely transparent. However, the product of isothermal reactions remains relatively turbid at the completion of the reaction, as will be discussed later in this paper. At this point it is important to state two preconditions for the evolution of a polymerizing inverse-macroemulsion into an polymer inverse-microemulsion. The particle diameter should be close to 100 nm, which is the approximate threshold between inverse-macroemulsions and inverse-microemulsions, and the temperature must increase during the reaction.

Elucidation of molecular structure

Figure 6 shows the trend in the weight-average molecular weight with conversion for a non-isothermal inverse-emulsion polymerization of acrylamide. Clearly, for this case, when unpurified acrylamide was employed, the molecular weight increased dramatically at conversions above 95%. This cannot be attributed to a change in the reaction environment causing a shift in the instantaneous molecular weight distribution, but rather must be interpreted as either long chain branching or intramolecular association. Further evidence that these polymers are either highly non-linear or associated is shown in the correlation plot of *Figure 7*. This compares the radius of gyration and molecular weights of solution polyacrylamides with inverse-microemulsion polymers. For the same molecular weight, the inverse-microemulsion polymers have significantly lower radii of gyration. We have also conducted static light scattering characterizations on heat treated samples in order to test whether the highly coiled or collapsed structure of these inverse-microemulsion polymers is a consequence of weak

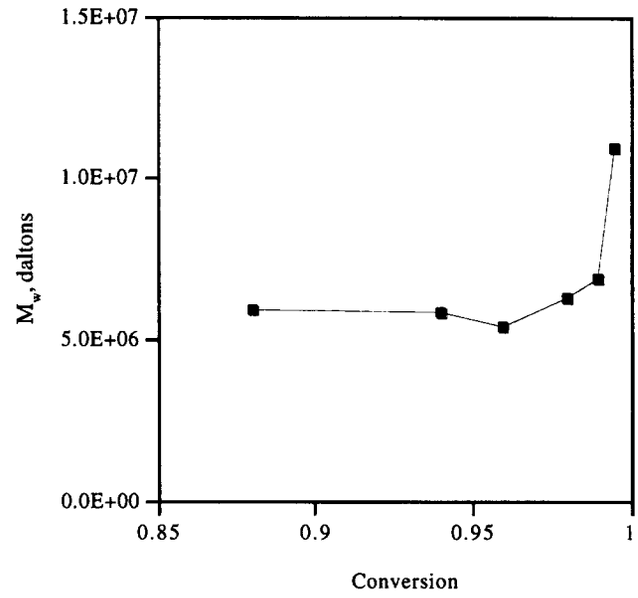

Figure 6 Experimental weight-average molecular weight ($\bar{M}_w$) as a function of conversion for a non-isothermal inverse-microemulsion polymerization of acrylamide. Experimental conditions are given in *Table 2* (MEM1)

bonded aggregates (polyacrylamide is known to H-bond and form reversible crosslinks) or covalent linkages[46]. These measurements found that both the radius of gyration and weight-average molecular weight were essentially unchanged (less than a 5% difference) when heat treated at 90°C for 30 min*. This supports a covalent

* This method has been recommended for acrylic water soluble polymers[47]

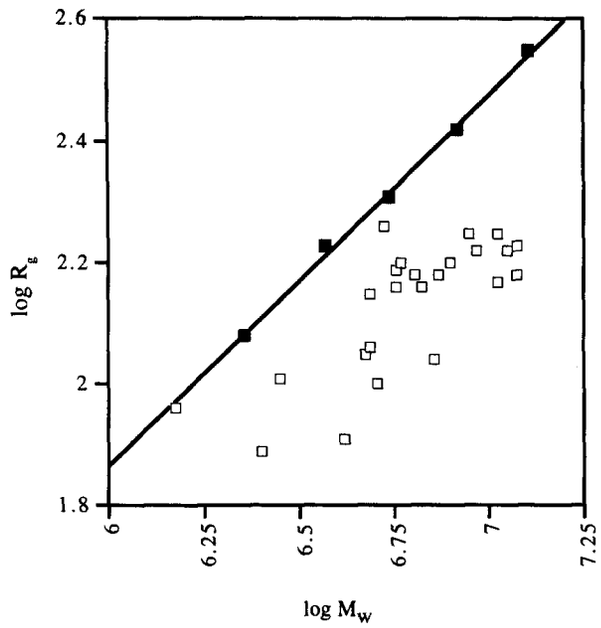

Figure 7 Correlation plot for solution (■) and inverse-microemulsion (□) polymerized acrylamide. The more compact nature of the inverse-microemulsion polymer is evident. Data for the solution polymers were taken from Kulicke *et al.*[71]

bonding hypothesis. However, a much more conclusive experimental investigation was recently conducted on the characterization of polyacrylamides in aqueous and organic media[48]. The 'apparent' molecular weight in 1.0 M NaCl of inverse-microemulsion polyacrylamides was found to be three times larger than in formamide. However, when a solution polymerized polyacrylamide was characterized in both solvents the molar masses were the same[48]. These indirect results indicate that the lower radius of gyration observed for inverse-microemulsion polyacrylamides are due to weak intramolecular interactions such 'reversible crosslinks'[46], which can be denatured with appropriate aprotic solvents. The development of a characterization method which could directly substantiate or refute the existence of covalent long chain branches would be helpful in resolving this debate.

The more compact nature of polymer chains in inverse-microemulsions compared with solution or inverse-emulsion polymerizations is likely to be exacerbated due to either local overheating, as was discussed above, or a small droplet size. For smaller particles the influence of interfacial reactions, such as those with the unsaturated groups on the oleate portion of the emulsifier, would increase[16–18]. Since these reactions are part of a long chain branching cascade, it is reasonable that polymers produced in smaller particles are more branched. Furthermore, the highly collapsed nature of a polyacrylamide chain in an inverse-microemulsion droplet will lead to a larger number of intramolecular interactions most likely in the form of hydrogen bonds.

Isothermal polymerizations with unpurified acrylamide

Figure 8 shows the change in viscosity and turbidity as a function of conversion for an isothermal polymerization. In comparison to *Figure 3*, the peak viscosity seems to occur at comparable conversions. However, the final inverse-latex remains relatively turbid throughout the course of the polymerization, in contrast to the non-isothermal experiments which clear near the end of the reaction. It is interesting to note that the particle size, molecular weight and radius of gyration are independent of both the peak temperature and whether the synthesis is performed under isothermal conditions, as is indicated in *Table 4*.

Heat transfer modelling of inverse-latex particles

In order to confirm that isothermal conditions could be established in water-in-oil polymerizations with particle diameters of the order of 150 nm, we have modelled the heat transfer from polymer containing droplets. This model found that three heat transfer domains exist which are distinguished by particle diameter thresholds. The derivation of this heat transfer model has been presented elsewhere[49]. For very small particle sizes (diameters less than approximately 12 nm), the particle can overheat due to a kinetic effect, as is illustrated in *Figure 9a*. This is the result of extremely large radical concentrations which are generated (close to 1 mol l^{-1}) if even one radical enters

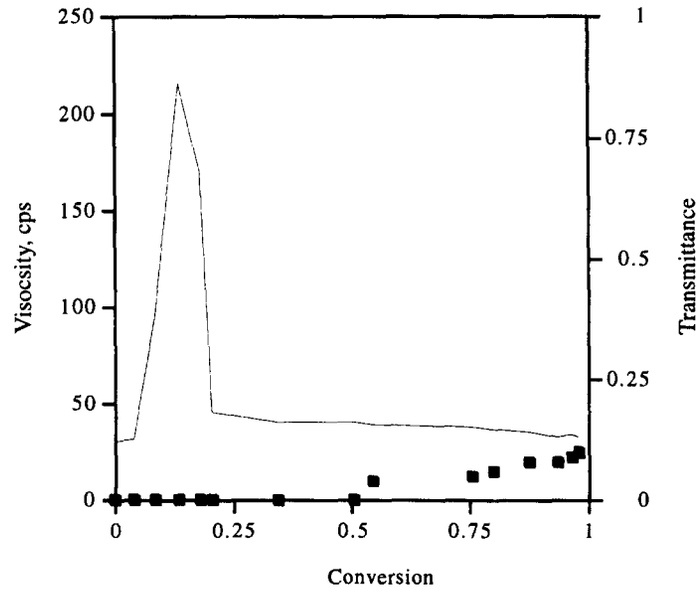

Figure 8 Shear viscosity (——) and turbidity (■) as a function of conversion for an isothermal inverse-microemulsion polymerization of acrylamide using V-70 as initiator. Experimental conditions: $T = 30°C$, $[M] = 3.29\,mol/L_w$, $[I] = 0.972\,mol/L_o$, HLB = 8.5, 8 wt% emulsifier, 50/50 wt% aqueous phase/oil phase. Emulsifier system: polyoxyethylene sorbitan trioleate/sorbitan monooleate

Table 4 Polymer characteristics from inverse-microemulsion polymerizations using unpurified acrylamide

System	Weight-average molecular weight (daltons × 10^7)	Radius of gyration (nm)	Average particle size (nm)
MEM1	1.02	168	150
MEM2	0.90	175	145
MEM3	0.98	155	160

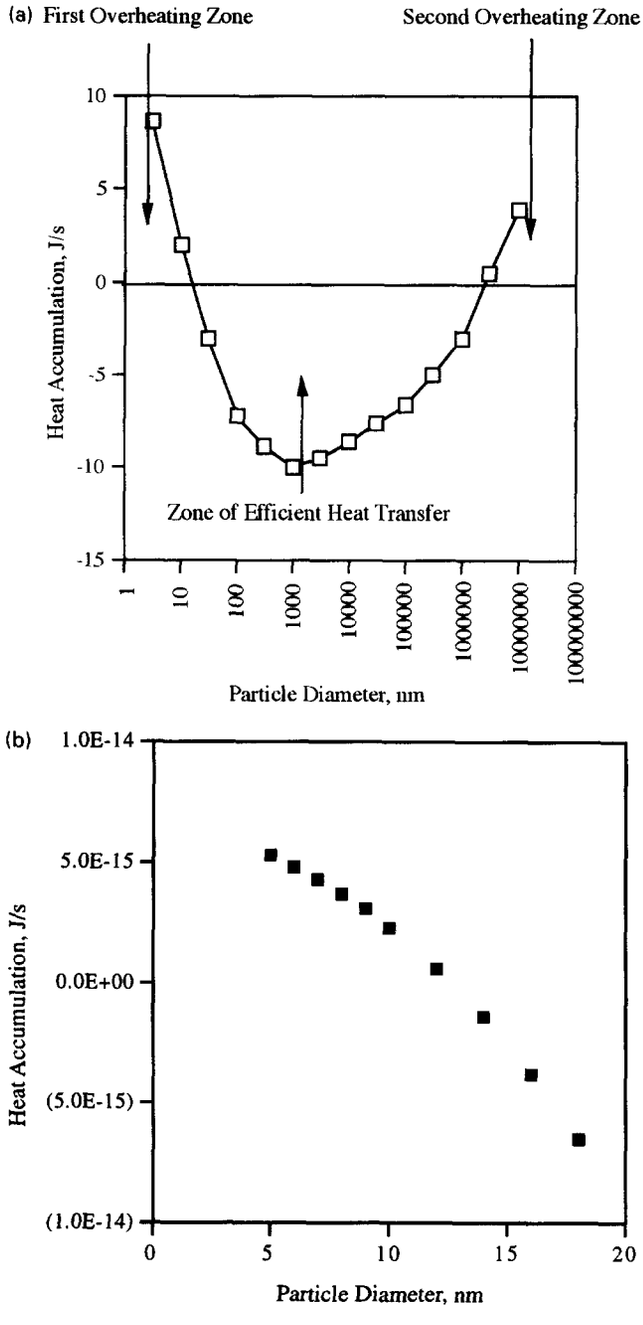

Figure 9 (a) The heat transfer from a spherical polymer particle is plotted as a function of particle size. Two domains exist where the heat generation exceeds the heat transfer to the surrounding fluid (Isopar-M). At very small particle sizes and for very large spheres the particles overheat. The former is a consequence of the high radical concentrations, which cause large heat generation rates, and the latter is due to a reduced surface-to-volume ratio. These calculations are based on a steady state model[49]. (b) Heat accumulation ($J s^{-1}$) as a function of the particle diameter (dp, nm). A critical dp of approximately 12 nm is observed below which the particles cannot dissipate all the reaction heat and overheat. The overall heat transfer coefficient for these simulations was assumed to be 500 $J m^{-2} s^{-1} K^{-1}$ [49].

the small particle. *Figure 9b* illustrates the overheating for small particles. A second domain of efficient heat transfer exists for intermediate particle diameters where the surface area is sufficient to dissipate the reaction heat. Clearly inverse-latices of the order of 150 nm lie in the domain of efficient heat transfer (*Figure 9a*). This implies that, if one is able to control the temperature of the continuous phase, the internal droplet temperature should be the same as that of the organic medium. A third domain exists at very large diameters, of the order of millimeters, where the surface-to-volume ratio is too small to transfer effectively the heat generated (*Figure 9a*).

SANS measurements

Physical and colloid chemists have studied microemulsions since the 1940s. Over the past 10 years detailed descriptions of the microstructure and dynamics of various microemulsions have been developed[50,51]. More recently, microemulsions have been recognized as providing a unique environment for synthetic chemistry[52,53]. However, while both the initial monomer microemulsions and the final polymer microemulsions have been well characterized, little is known about the transformation of microemulsions or inverse-microemulsions throughout the polymerization. As we have shown earlier in this paper, a complex variety of rheological, optical and rheo-optical changes are observable during the course of a reaction.

SANS is a very powerful tool for the determination of the shape and size of particles of typical colloidal dimensions. Similar studies involving related systems have been published including inverse AOT micelles[54-57] AOT/toluene/(water + acrylamide) micellar solutions[58] and aqueous ampholytic copolymers prepared by inverse-microemulsion[59]. Based on this, SANS was thought to be a potentially useful tool for the characterization of time and conversion dependent static properties of these inverse-microemulsions.

Figure 10 shows the experimental SANS data as a function of conversion when the initial monomer system is outside the inverse-microemulsion domain. Clearly, the intensity spectra of each individual sample are practically superimposed, indicating that both the form and structure factors are independent of conversion. The shape of the curve suggests this system is particulate and the size of the particles does not change with conversion. Applying the Guinier approximation [using $I(Q)$ at very low values of Q][60], a radius of gyration of 77 nm is obtained for the particles and this is invariant to conversion as is shown in *Figure 11*. This is in excellent agreement with the value for the particle diameter ($\approx$ 155 nm) obtained for most of our final latices by dynamic light scattering measurements which are reported in this paper.

Similarly, in an effort to obtain the particle diameter from the total intensity data [$I(Q)$ *versus* Q], several models were used. The best results were found using a polydisperse spherical particles model[61]. *Figure 12* shows the measured and fitted intensity spectra for this model. The equation used in this calculation is given by

$$I(Q) = AN_P P(Q)S(Q) + N_P\Delta(Q) + B \qquad (1)$$

where A is a scaling parameter that considers uncertainty in the calibration, N_P is the number density of particles, $P(Q) = \langle F(Q)\rangle^2$ is the scattering function of a single particle and provides information on internal organization, $S(Q)$ is the structure function which arises from

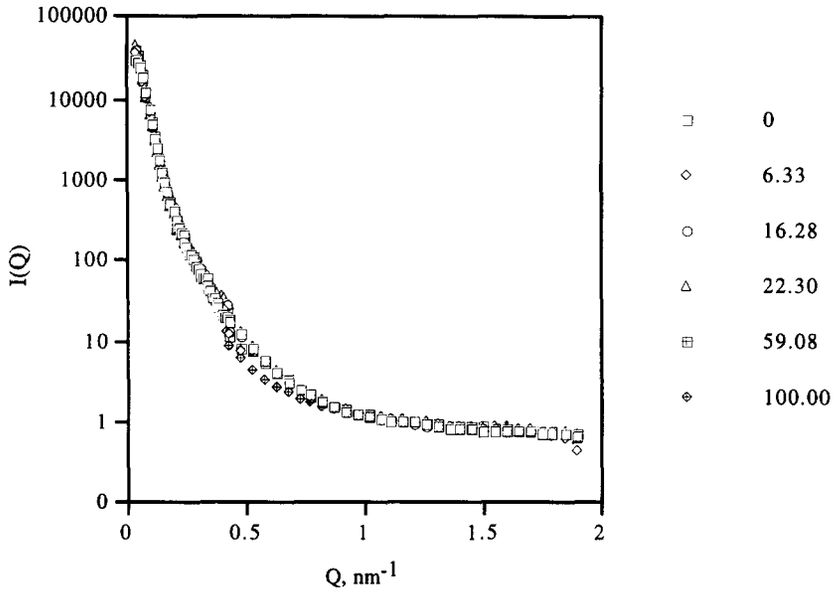

Figure 10 Experimental SANS spectra as a function of conversion for heterophase water-in-oil polymerizations outside the inverse-microemulsion domain. Experimental conditions for the polymerizations are given in *Table 3* (Experiment 9)

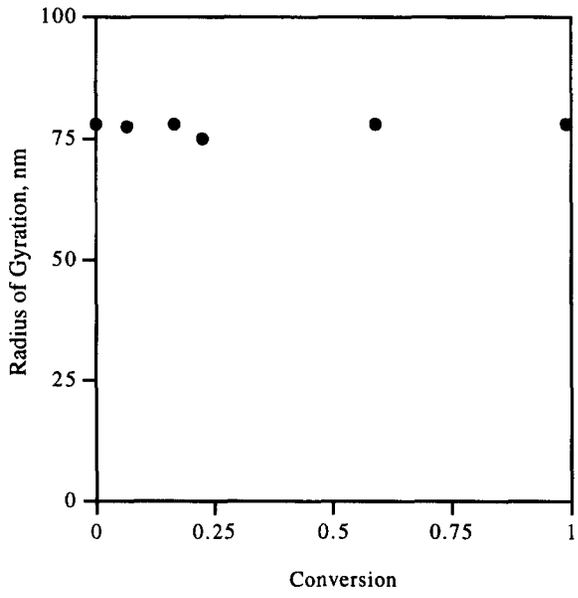

Figure 11 Radius of gyration for the spherical particles *versus* conversion. The radius of gyration was calculated according to the Guinier approximation. Experimental conditions for the polymerizations are given in *Table 3* (Experiment 9)

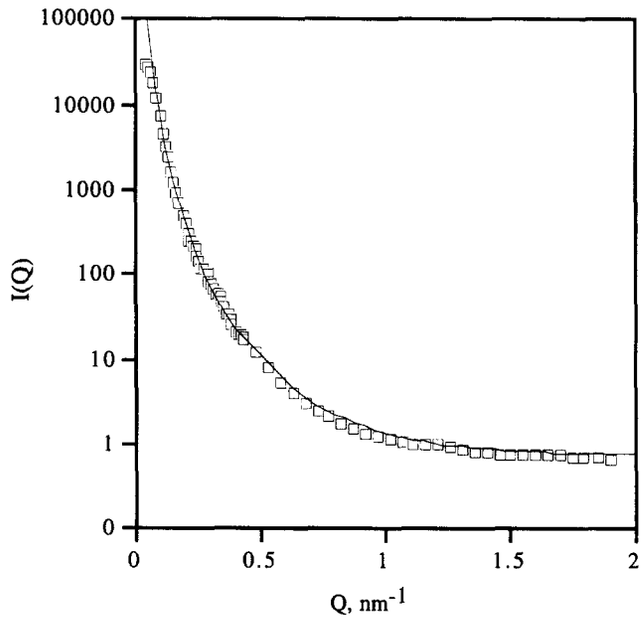

Figure 12 Experimental SANS (□) for the initial monomeric system. The solid line represents the calculated curve for a polydisperse spherical particles model. The initial system is located outside the inverse-microemulsion domain

interparticle scattering, $\Delta(Q) = \langle F(Q)^2 \rangle - \langle F(Q) \rangle^2$ is a term which takes into consideration deviation from sphericity and/or from monodispersity, and B is a background term. Here, the scattering density of the core was taken as the sum of the individual density contributions of acrylamide and D_2O multiplied by their molar ratios relative to D_2O, the scattering of the shell was calculated as the sum of the individual density contributions of each of the hydrophilic parts of the surfactants multiplied by their molar ratios relative to D_2O, and the scattering density of the solvent was approximated as the scattering density of decane. *Table 5* lists the parameters used/obtained in the fitting. Obviously, the fit is excellent, indicating that our polymerizing system consists of polydisperse spherical droplets. The estimated radius of gyration of the particles was 73 nm, and the polydispersity (according to a Schultz distribution) was 53.22. The presence of small particles such as inverse-micelles was not detected. Therefore, these polymerization systems seem to follow a macroemulsion-like mechanism where the particle diameter is invariant of conversion.

The experimental SANS data as a function of conversion when the initial monomer system is inside the microemulsion domain is shown in *Figure 13*. An evolution of particle shape and possibly also of particle size with conversion is clearly observed. The analysis of these data will be reported in a future publication.

Table 5 Parameters regressed in the fitting of radius of gyration from the total intensity spectra (Experiment 9)

Parameter	Value
Scale factor	1.0
Background	0.7
Inner radius (Å)	558.9
Total radius (Å)	730.0
Polydispersity	53.22

Isothermal polymerizations with purified acrylamide

The rate of polymerization and weight-average molecular weight for the isothermal heterophase polymerizations with purified acrylamide are shown in *Figure 14* as a function of the initiator concentration. The polymerization rate is observed to vary with respect to initiator concentration to the 1.0 power, as was also observed in inverse-macroemulsions[6,7–9,16–18,62]. Carver *et al.*[63] have also found a first-order dependence in inverse-microemulsions. Most authors have attributed this behaviour to the existence of a unimolecular

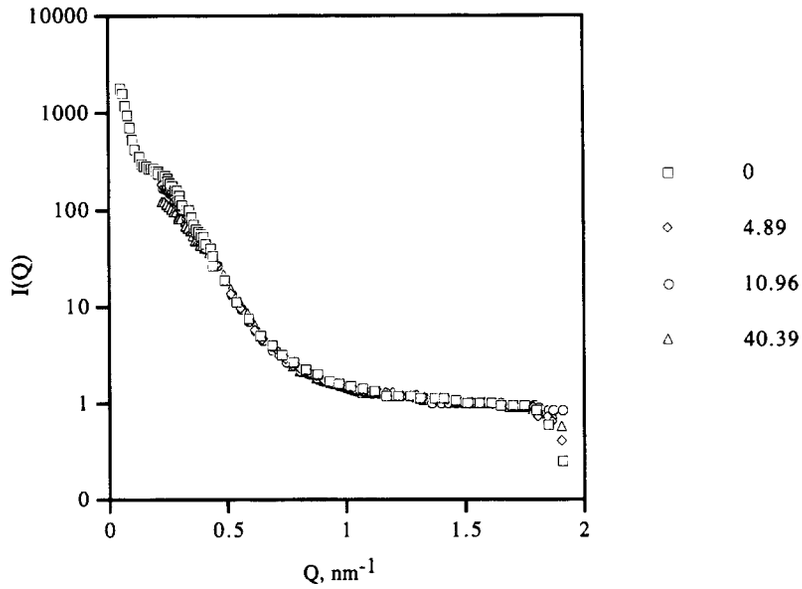

Figure 13 Experimental SANS spectra as a function of conversion for heterophase water-in-oil polymerizations inside the inverse-microemulsion domain. Experimental conditions for the polymerizations are given in *Table 3* (Experiment 10)

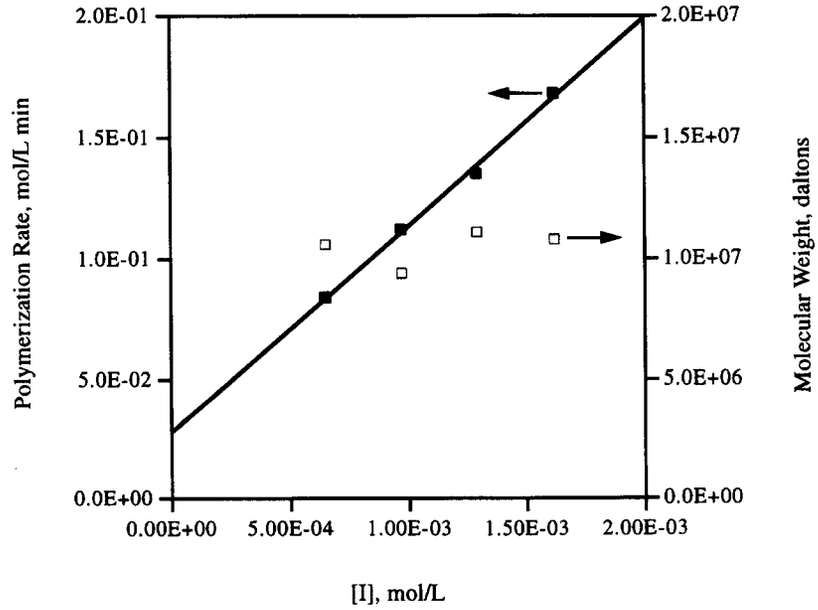

Figure 14 Rate of polymerization (■) and weight-average molecular weight (□) *versus* molar initiator concentration of initiator (V-70) for the inverse microemulsion polymerization of acrylamide. The continuous line represents the linear regression line. Experimental conditions: $T = 30°C$, $[M] = 3.29\,mol/L_w$, HLB = 7.8, 8 wt% emulsifier, 50/50 wt% aqueous phase/oil phase. Emulsifier system: polyoxyethylene sorbitan trioleate/sorbitan monooleate

termination step with either emulsifier, a solvent phase species or impurities. The molecular weight is also essentially independent of the initiator level, within the limitations of experimental reproducibility. We believe these data are consistent with a mechanism where the bimacromolecular disproportionation termination reaction is very uncompetitive compared with transfer reactions to monomer and emulsifier.

Mechanism

Based on the experimental evidence presented in the preceding paragraphs (SANS and rate dependence), a mechanism for this hybrid inverse-emulsion/inverse-microemulsion polymerization process will be proposed in this section. Similar mechanisms have been developed for the inverse-macroemulsion polymerization of acrylamide[16–18,41] and inverse-microemulsion polymerization of acrylic water soluble monomers[64]. The mechanism is consistent with the discussion presented earlier in this paper and includes a heterophase reaction scheme with initiation and propagation in the continuous phase, partitioning and oligoradical precipitation between the continuous and aqueous phases, and a classical free-radical reaction scheme in the acrylamide–water particles. The known mechanistic characteristics of inverse-microemulsions such as the co-surfactant nature of acrylamide and the interfacial emulsifier and monomer reactions have also been incorporated. Termination by disproportionation is in competition with transfer to monomer and emulsifier. Since the particle diameter is of the order of 155 nm, the potential for a chain to polymerize all the monomer in a particle prior to termination is not included[29]. Simple kinetic calculations based on the total monomer in a particle indicate that this would occur for particle diameters below 40 nm, given the values of k_p, k_{td} and k_{fm} for acrylamide polymerizations.

Organic phase reactions:

$$I \xrightarrow{k_d} 2R^{\bullet}_{in,O} \quad (2)$$

$$R^{\bullet}_{in,O} + E_O \xrightarrow{k_1} \text{inert products} \quad (3)$$

$$R^{\bullet}_{in,O} + HC \xrightarrow{k_4} \text{inert products} \quad (4)$$

$$R^{\bullet}_{in,O} + M_O \xrightarrow{k_p} R^{\bullet}_{1,O} \quad (5)$$

$$R^{\bullet}_{r,O} + M_O \xrightarrow{k_p} R^{\bullet}_{r+1,O} \quad (6)$$

where $R^{\bullet}_{in,O}$, HC, E_O, M_O and $R^{\bullet}_{r,O}$ are the symbols for primary radicals, hydrocarbon, emulsifier, monomer and macroradicals in the oil phase. The subscript 'o' designates an organic phase species.

Heterophase mass transfer:

$$R^{\bullet}_{in,O} \xrightarrow{k_r} R^{\bullet}_{in,W} \quad (7)$$

$$R^{\bullet}_{r,O} \xrightarrow{k_{r,r}} R^{\bullet}_{r,W} \quad (8)$$

$$M_O \overset{\Phi_m}{\Longleftrightarrow} M_W \quad (9)$$

where the subscript 'w' denotes a water phase species, $k_{r,r}$ is the mass transfer constant of an oligoradical of length r, which will tend to k_r at small chain lengths, and Φ_m is the equilibrium monomer partition coefficient.

Aqueous phase reactions:

Propagation:

$$R^{\bullet}_{in,W} + M_W \xrightarrow{k_p} R^{\bullet}_{1,W} \quad (10)$$

$$R^{\bullet}_{r,W} + M_W \xrightarrow{k_p} R^{\bullet}_{r+1,W} \quad (11)$$

$$''R^{\bullet}_{r,W} + M_W \xrightarrow{k_p} ''R^{\bullet}_{r+1,W} \quad (12)$$

Reactions of surface active emulsifiers and emulsifier radicals:

$$R^{\bullet}_{r,W} + \Gamma_E \xrightarrow{k_{fe}} P_r + E^{\bullet} \quad (13)$$

$$''R^{\bullet}_{r,W} + \Gamma_E \xrightarrow{k_{fe}} ''P_r + E^{\bullet} \quad (14)$$

$$E^{\bullet} + M_W \xrightarrow{k_p} ''R^{\bullet}_{1,W} \quad (15)$$

$$E^{\bullet} + HC_{imp} \xrightarrow{k_5} \text{inert products} \quad (16)$$

Transfer to monomer:

$$R^{\bullet}_{r,W} + M_W \xrightarrow{k_{fm}} P_r + R^{\bullet}_{1,W} \quad (17)$$

$$''R^{\bullet}_{r,W} + M_W \xrightarrow{k_{fm}} ''P_r + R^{\bullet}_{1,W} \quad (18)$$

Termination:

$$R^{\bullet}_{r,W} + R^{\bullet}_{s,W} \xrightarrow{k_{td}} P_r + P_s \quad (19)$$

$$''R^{\bullet}_{r,W} + R^{\bullet}_{s,W} \xrightarrow{k_{td}} ''P_r + P_s \quad (20)$$

$$''R^{\bullet}_{r,W} + R^{\bullet}_{s,W} \xrightarrow{k_{td}} ''P_r + ''P_s \quad (21)$$

Long chain branching:

$$''P_{r,W} + R^{\bullet}_{s,W} \xrightarrow{k^*} R^{\bullet}_{r+s,W} \quad (22)$$

$$''P_r, W + ''R^{\bullet}_{s,W} \xrightarrow{k^*} ''R^{\bullet}_{r+S,W} \quad (23)$$

where $''R^{\bullet}$ and $''P_r$ are macroradicals and dead polymer chains containing residual functional groups which can participate in long chain branching reactions, Γ_E is the total surface concentration of emulsifier, $E^{\bullet}$ is the symbol for an emulsifier radical, and HC_{imp} represents hydrocarbon-phase impurities or radicals. The subscript 'w' designates an aqueous phase species.

It is important to note that this mechanism describes the reaction of a single emulsifier, whereas the experimental results in this paper involved a surfactant blend. Rigorously, each functional group on both the polyoxyethylene sorbitan derivatives and the sorbitan fatty acid esters has a unique reactivity to radicals (steps 3 and 13). However, regressing independent kinetic estimates of an extensive list of such transfer reactions would not be possible from a numerical simulation of the kinetic model. Therefore, we have

estimated the transfer coefficients (k_1, k_{fe}) as an averaged value for all the function groups on the emulsifier blend. Similarly, the emulsifier radical generated from such a reaction ($E^{\bullet}$), *de facto*, represents radicals on either the polyoxyethylated sorbitan derivatives or the sorbitan fatty acid ester. However, it is treated as a single species in order to permit parameter estimation. It remains the topic of a future study to map the reactivity of functional groups on various water-in-oil surfactants.

Kinetic modelling

The preceding mechanism can be reduced to a set of differential and algebraic equations which describe each reactive species concentration and molecular weights ($\bar{M}_N$ and $\bar{M}_w$). The resulting kinetic modelling predicts the polymerization rate behaviour[16–18,65]:

$$R_p = \frac{2fk_d k_p[I][M]}{(1-f_e)k_{fe}\Gamma_E} \tag{24}$$

where f and f_e are the efficiencies of radicals generated by thermal decomposition and macromolecular termination with emulsifier[16–18]:

$$f = \frac{1}{1+\frac{\Phi_r}{k_r^*}\left(\frac{k_4[HC]}{a_{sp}}+\frac{k_1[E_0]}{a_{sp}}\right)} \cdot \frac{V_O}{V_w} \tag{25}$$

$$f_e = \frac{1}{1+\frac{k_5[HC_{imp}]}{k_p[\bar{M}_w]}} \tag{26}$$

Φ_r and a_{sp} are the partitioning coefficient of oligoradicals between the organic and aqueous phases and the specific interfacial area ($m^2 l^{-1}$ of organic phase), respectively.

Using the method of moments, the following equations have been derived for the number and weight average molecular weights ($\bar{M}_N$ and $\bar{M}_w$)[65]:

$$\bar{M}_n = M_m \frac{Q_1}{Q_O}$$

$$\bar{M}_w = M_m \frac{Q_2}{Q_1}$$

where M_m is the molecular weight of the monomer, and Q_i is the ith moment of the distribution of polymer molecules[65].

Parameter estimation

In order to apply the kinetic model to specific inverse-microemulsion polymerizations of acrylamide, several rate, mass transfer and partition coefficients are needed. In the absence of available literature values these must be estimated from experimental data. These parameters have been determined by non-linear weighted least squares regression using Marquardt's procedure to minimize the sum of squares of the residuals. The total residual is comprised of two independent measurements, conversion and weight average molecular weight which are weighted by the reciprocal of their variances as follows:

$$\text{Min}\sum_{i=1}^{n}\left[\left|\left(\frac{X_{i,p}-X_{i,d}}{\sigma_{x,i}^2}\right)\right|+\left|\frac{MW_{i,p}-MW_{i,d}}{\sigma_{MW,i}^2}\right|\right]^2$$

where n is the number of repetitions, and $X_{i,p}$ and $X_{i,d}$ are the predicted and measured conversion, respectively. $MW_{i,p}$ and $MW_{i,d}$ are the model and experimental weight average molecular weights, and $\sigma_{x,i}^2$ and $\sigma_{MW,i}^2$ are the variance of the ith conversion and molecular weight measurements, respectively. Only the experimental conversion and weight-average molecular weight data for the polymerizations conducted under isothermal conditions were used in the parameter estimation. The conclusions from the parameter estimation are summarized below:

(1) The individual parameters values for Φ_r and k_r^* in equation (25) are indeterminate since this would require experimentation into the partitioning and mass transfer of primary radicals between the oil and water phases. While this research is certainly warranted, it would be extremely non-trivial to perform on reactive intermediates. The exact value of [HC] is also unknown since Isopar-M is a mixture of high boiling point straight chain alkanes with some aromatics. For this reason, these parameters were fitted as a group of constants, as they

Table 6 Summary of parameter values used in the kinetic model

Parameter	Value	95% Confidence limit	95% Confidence limit	Units	Reference
k_d	6.18×10^{15} exp $(-27400/RT)$			min^{-1}	66
k_p	9.9×10^7 exp $(-2743/RT)$			$l\ mol^{-1}$ min^{-1}	67–69
$k_t^{1/2}$	9.192×10^4 exp $(-741/RT)$			$l\ mol^{-1}$ min^{-1}	67–69
k_{fm}	5.73×10^8 exp $(-10438/RT)$			$l\ mol^{-1}$ min^{-1}	70
A	$11.22-1.67 \times 10^{-2}\ T$			Dimensionless	70
$K_{fe}\Gamma_E$	3.4×10^7 exp $(-4472/T)$				
$k_{fe}\Gamma_E$	16.898, at 35°C	26.98	6.816	min^{-1}	This work
	13.416, at 30°C	16.755	10.007		
	10.387, at 25°C	12.141	8.634		
f_e	0.701, at 35°C	0.866	0.536	Dimensionless	This work
	0.510, at 30°C	0.633	0.387		
	0.295, at 25°C	0.348	0.241		

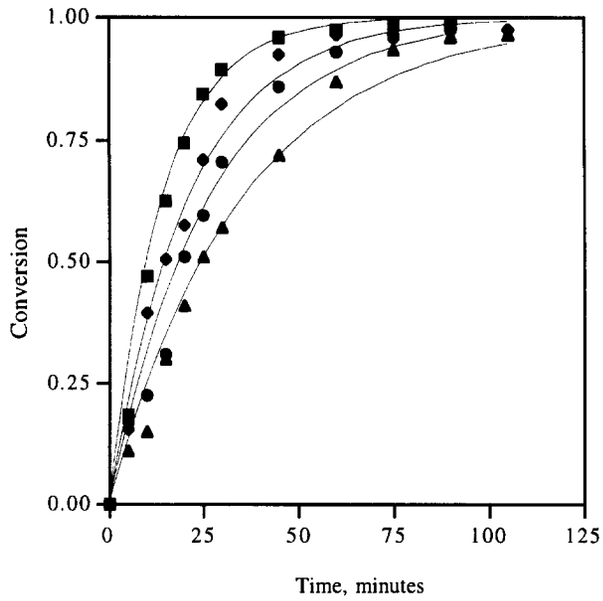

Figure 15 Experimental and predicted conversion (——) *versus* time for the inverse-microemulsion polymerization of acrylamide at various molar initiator concentrations (V-70): 2.43 mmol/L_o (■), 1.62 mmol/L_o (◆), 1.29 mmol/L_o (●), 0.972 mmol/L_o (▲). Experimental conditions: T = 30°C, [M] = 3.29 mol/L_W, HLB = 7.8, 8 wt% emulsifier, 50/50 wt% aqueous phase/oil phase. Emulsifier system: polyoxyethylene sorbitan trioleate/sorbitan monooleate

appear in the kinetic model:

$$\frac{\Phi_r}{k_r^*}\left(\frac{k_4[HC]}{a_{sp}}+\frac{k_1[E_0]}{a_{sp}}\right)$$

The regressed value of this grouped parameter was very small (10^{-4}) at 30°C, which renders f, the efficiency of initiation, very close to unity (0.99–1.0). This indicates that the consumption of radicals in the organic phase by either the hydrocarbon or the soluble emulsifier is practically zero. This is reasonable for the following reasons: (i) the level of impurities is believed to be very low due to the use of purified and peroxide-free emulsifiers, and (ii) the specific interfacial area a_{sp} of the particles is large and approximately 100 times that for a typical 1 μm particle produced by inverse-macroemulsion polymerization. Therefore, the capture of radicals by the small inverse-microemulsion droplets is very efficient, in analogy to the kinetic process occurring in direct emulsion polymerization. It is interesting to note that the efficiency of initiation in inverse-macroemulsions stabilized with sorbitan monooleate was in the 5–20% range[16–18,65], far below what is observed for these inverse-microemulsions.

(2) The transfer to emulsifier constant and equilibrium surface emulsifier concentration were determined as a lumped parameter ($k_{fe}\Gamma_E$) at each polymerization temperature used (25, 30 and 35°C). The temperature dependence of this lumped parameter follows the Arrhenius equation with a relatively moderate activation energy, as shown in *Table 6*. A low positive activation energy is typical of termination reactions, and similar values have been reported for transfer to sorbitan monooleate in inverse-suspension[16–18,65].

(3) The efficiency of initiation of emulsifier radicals increases, approximately linearly, with temperature. This is likely the result of a higher aqueous phase solubility or diffusion coefficient as the temperature rises. This would increase the probability of a radical reacting with acrylamide at the interface or in aqueous solution prior to exodiffusion into the organic phase where it would terminate.

Kinetic model predictions

Effect of initiator concentration. Figure 15 shows the experimental data and kinetic model predictions of the conversion *versus* time behaviour as a function of the initiator concentration. A constant initial polymerization rate is observed up to 50–60% accompanied by a mild gel effect. The initial polymerization rate increases with increasing initiator level, which clearly demonstrates that the reaction rate is an intrinsic one and is

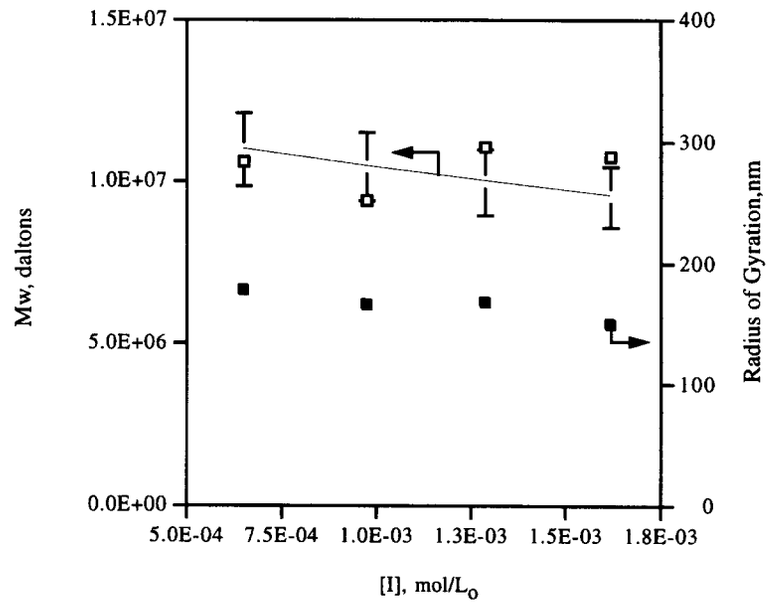

Figure 16 Experimental weight-average molecular weight ($\bar{M}_W$) (□), predicted ($\bar{M}_W$) (——) and experimental radius of gyration (■) *versus* initiator concentration for an inverse-microemulsion polymerization of acrylamide using V-70 as initiator. Experimental conditions: T = 30°C, [M] = 3.29 mol/L_W, HLB = 7.8, 8 wt% emulsifier, 50/50 wt% aqueous phase/oil phase. Emulsifier system: polyoxytheylene sorbitan trioleate/sorbitan monooleate

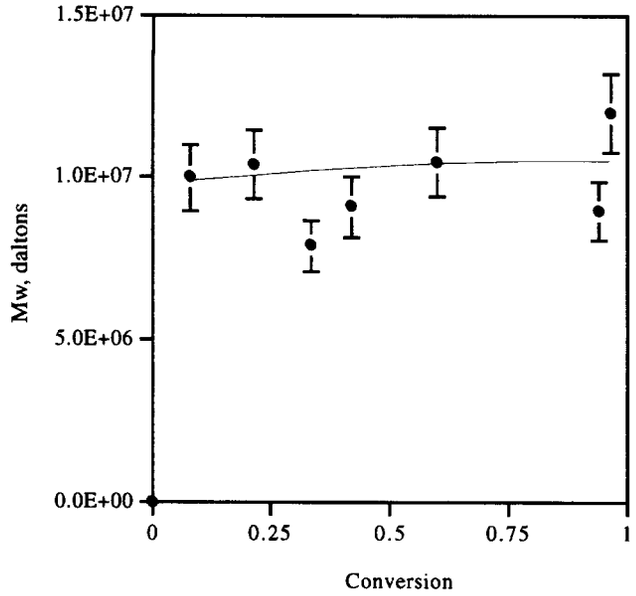

Figure 17 Experimental (■) and predicted weight-average molecular weight ($\bar{M}_W$) (——) *versus* conversion for a inverse-microemulsion polymerization of acrylamide using V-70 as initiator. Experimental conditions: $T = 30°C$, $[M] = 3.29\,mol/L_W$, $[I] = 0.972\,mmol/L_O$, HLB = 7.8, 8 wt% emulsifier, 50/50 wt% aqueous phase/oil phase. Emulsifier system: polyoxyethylene sorbitan trioleate/sorbitan monooleate

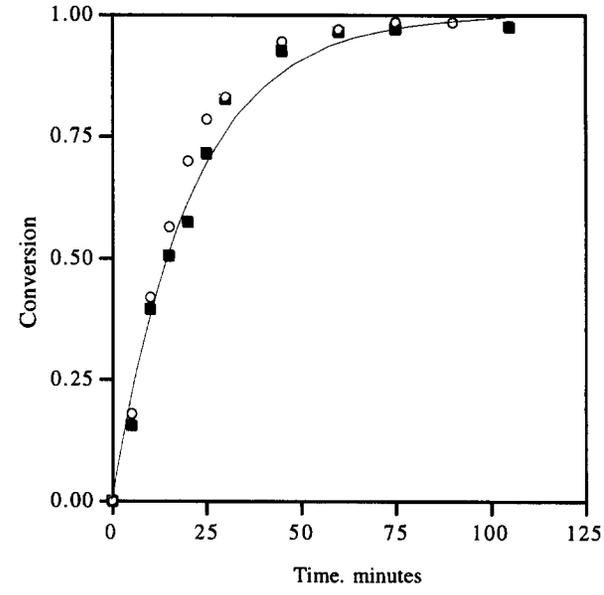

Figure 19 Experimental and predicted conversion (——) *versus* time for the inverse-microemulsion polymerization of acrylamide using V-70 as initiator at two HLBs: 8.2 (■) and 7.8 (□). Experimental conditions: $T = 30°C$, $[M] = 3.29\,mol/L_W$, $[I] = 1.62\,mmol/L_O$, 8 wt% emulsifier, 50/50 wt% aqueous phase/oil phase. Emulsifier system: polyoxyethylene sorbitan trioleate/sorbitan monooleate

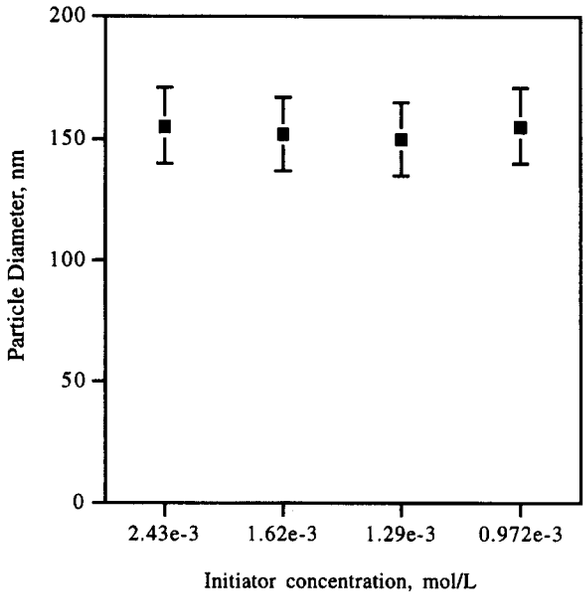

Figure 18 Average particle diameter (dynamic light scattering) *versus* initiator concentration for inverse-microemulsion polymerization of acrylamide using V-70 as initiator. Experimental conditions: $T = 30°C$, $[M] = 3.29\,mol/L_W$, HLB = 7.8, 8 wt% emulsifier, 50/50 wt% aqueous phase/oil phase. Emulsifier system: polyoxyethylene sorbitan trioleate/sorbitan monooleate

caused by the thermal decomposition of the initiator. Moreover, the kinetic model can predict the experimental data very well over the range of initiator concentrations studied. Similarly, the model gives good estimates of the final weight-average molecular weight ($\bar{M}_W$) at different initiator concentrations (*Figure 16*) and the trend in molecular weight with conversion (*Figure 17*). The molecular weights are only very slightly dependent on conversion, which indicates that the transfer to the monomer step is controlling the molecular weight. The average particle diameter of the final inverse-microemulsion latices produced herein, and measured by dynamic light scattering, was found to be practically independent on the initiator concentration with values in the range of 155 nm as illustrated in *Figure 18*. This value, as indicated earlier, is in excellent agreement with the particle diameter found in our SANS experiments.

Figure 16 also shows the radius of gyration for these polymerizations as a function of the initiator concentration. The radius of gyration mildly decreases, within the limitations of experimental reproducibility, with the initiator level, as is normally observed in free radical reactions, dominated by transfer to monomer.

Effect of HLB. Figure 19 shows that the rate of the polymerization is largely uninfluenced by the HLB of the system over the range 7.8–8.2. This limited range was delineated by the desire to conduct these polymerizations isothermally. At higher HLBs, as was mentioned previously, the viscosity increase near the phase inversion was sufficiently large to cause the temperature of the whole reaction mixture to rise. The independence of the polymerization rate on the HLB of the initial system is due to the invariance of the particle diameter of these systems to the reaction conditions, as is observed during polymerizations using SANS (*Figures 20* and *21*). As expected, the data for molecular weight and radius of gyration were also found to be independent of HLB.

Temperature effects. The kinetic model also gives reasonable predictions of the conversion and weight-average molecular weight at temperatures between 25 and 35°C, as shown in *Figures 22* and *23*, respectively. The strong influence of the activation energy for the decomposition of the initiator is evident, as is standard in free radical processes. The weight-average molecular weight shows only a mild dependence on temperature. This is atypical of polymerizations controlled by transfer

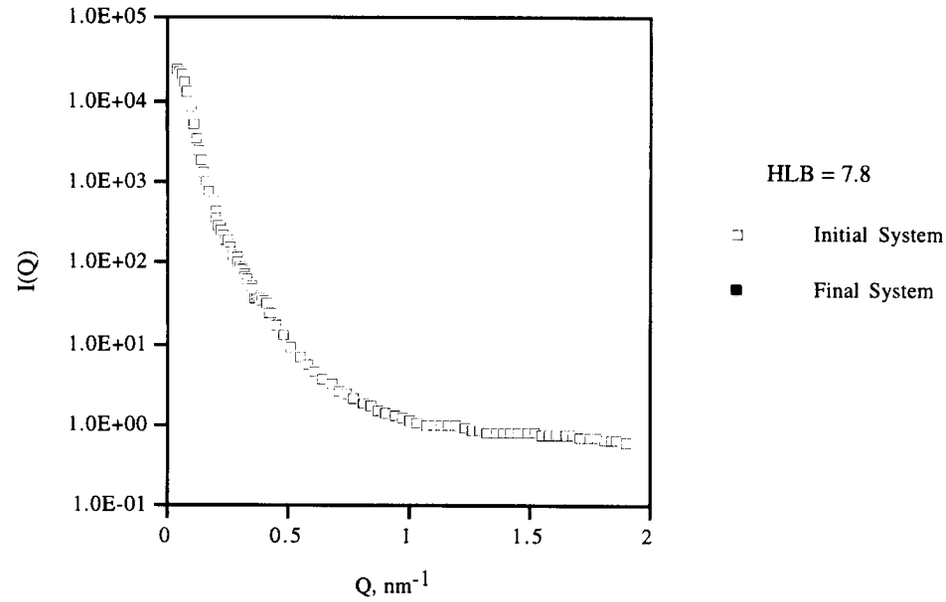

Figure 20 Experimental SANS spectra as a function of conversion for heterophase water-in-oil polymerizations outside the inverse-microemulsion domain at a HLB of 7.8. Experimental conditions for the polymerizations are given in *Table 3* (Experiment 6)

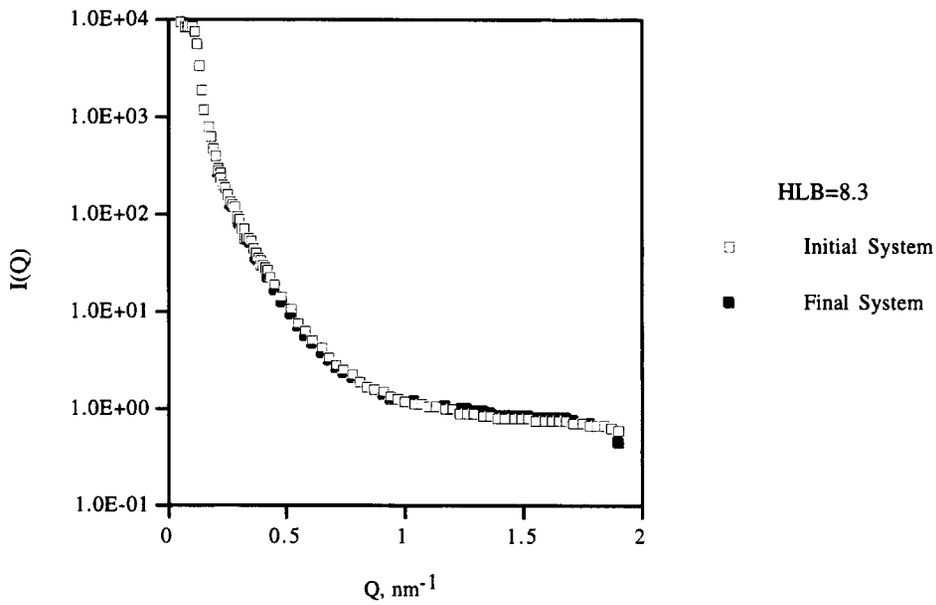

Figure 21 Experimental SANS spectra as a function of conversion for heterophase water-in-oil polymerizations outiside the inverse-microemulsion domain at a HLB of 8.3. Experimental conditions for the polymerizations are given in *Table 3* (Experiment 3)

to monomer and is likely due to the small range in temperatures investigated (10°C). Since some of the macroradicals are terminated through an interfacial reaction with emulsifier, a second effect could be due to the low activation energy for this reaction (*Table 5*) and dependence of transfer to interfacial emulsifier on the particle diameter[16–18,64]. Given that the particle diameter is observed to be invariant with temperature, between 25 and 35°C, the transfer to emulsifier rate constant should also be relatively temperature insensitive, as is experimentally observed.

CONCLUSIONS

Heterophase water-in-oil polymerizations of acrylamide were conducted under various conditions in the presence of blends of non-ionic stabilizers at moderate concentrations. At a position on the phase diagram outside the inverse-microemulsion domain, yet very close to the inverse-macroemulsion/inverse-microemulsion phase boundary, these systems are turbid, viscous and unstable at the early and intermediate stages of the polymerization. By the completion of the reaction these systems become stable and inviscid inverse-latices. They can also evolve into transparent systems at the final stages of the reaction provided that the polymerization is conducted under non-isothermal conditions. At moderate HLBs, the increase in viscosity observed early during the polymerization can be explained in terms of the polymer formed and is partially located in the continuous phase (phase inversion). At high HLBs, however, the viscosity increase can be explained by the formation of liquid crystal

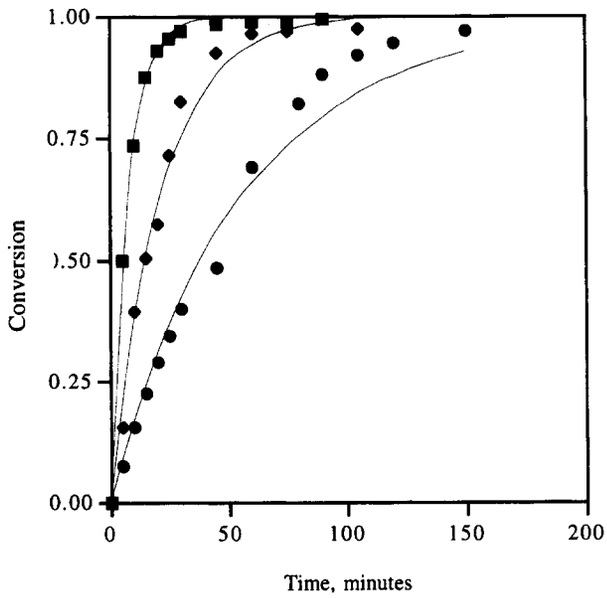

Figure 22 Experimental and predicted conversion (——) *versus* time for the inverse-microemulsion polymerization of acrylamide using V-70 as initiator as a function of temperature: 35°C (■), 30°C (◆) and 25°C (●). Experimental conditions: [M] = 3.29 mol/L_W, [I] = 1.62 mmol/L_O, HLB = 7.8, 8 wt% emulsifier, 50/50 wt% aqueous phase/oil phase. Emulsifier system: polyoxyethylene sorbitan trioleate/sorbitan monooleate

structures. The final transparency of the non-isothermal systems is likely caused by one of two effects. (1) Due to the location of the initial system close to the inverse-macroemulsion/inverse-microemulsion phase boundary, and the small particle size, a reduction in the interfacial tension, due to an increase in the internal droplet temperature, can cause an outward movement in the inverse-microemulsion phase sufficient to engulf our initial point. In this case the polymerization takes place through a 'hybrid inverse-macroemulsion/inverse-microemulsion mechanism'. (2) The transparency can be an artefact due to the change in the refractive index with the conversion of monomer into polymer.

SANS studies of the initial monomer and reacting systems outside the inverse-microemulsion domain of the phase diagram show that these systems are particulate with a particle diameter of 155 nm, independent of conversion. The SANS intensities can be modelled using a polydisperse spherical particles model. Therefore, these heterophase water-in-oil polymerization systems seem to follow an inverse-macroemulsion-like mechanism. The inverse-microemulsion polyacrylamides have a low radius of gyration in aqueous solutions relative to solution and inverse-macroemulsion polymers of the same weight-average molecular weight. This is likely due to a large number of intramolecular interactions (such as hydrogen bonding) which are induced by the collapsed nature of the polymer chains in the inverse-microemulsion droplets. The weight-average molecular weight, radius of gyration and particle diameter of the final latex are relatively independent of the polymerization conditions such as initiator level, HLB and temperature. The physical changes occurring during polymerization do not affect the final properties of the latex; however, they affect engineering parameters such as the heat transfer coefficient and the final state of the product. If the viscosity increase is observed too late in the process, the system is usually unable to transform itself into a transparent non-settling microemulsion.

From a kinetic point of view, the molecular weights of these systems are controlled by transfer to monomer while transfer to interfacial emulsifier is the polymerization rate controlling step. A reaction mechanism consisting of a number of elementary reactions has been proposed for these heterophase water-in-oil polymerizations. The agreement with the experimental data is found to be good at different levels of initiator, HLBs and temperature.

Despite the limitations of this heterophase water-in-oil polymerization process (the moderate emulsifier levels required, low radius of gyration and its inability to increase the molecular weight beyond 10^7 daltons), this polymerization process can produce final latices that are transparent and low-settling with small particles

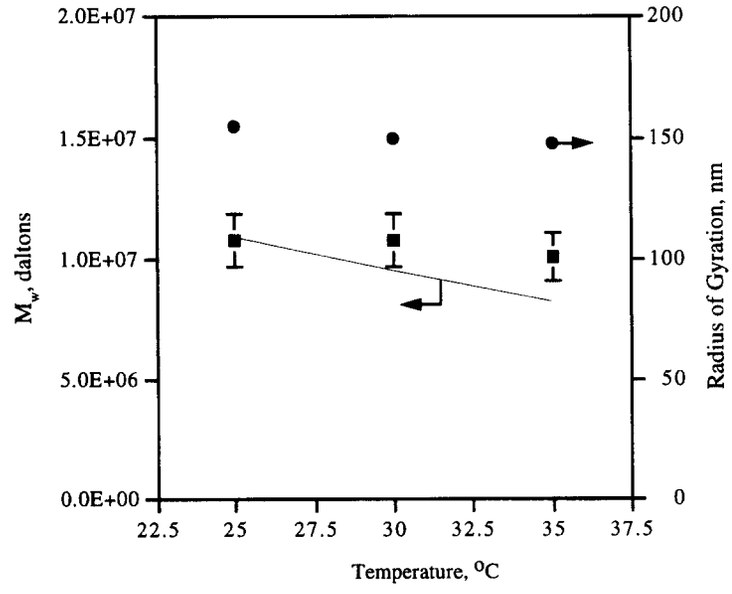

Figure 23 Experimental (discrete symbols) weight-average molecular weight ($\bar{M}_W$), (■) predicted ($\bar{M}_W$) (——) and experimental radius of gyration (●) *versus* polymerization temperature for inverse-microemulsion polymerizations of acrylamide using V-70 as initiator. Experimental conditions: T = 30°C, [M] = 3.29 mol/L_W, HLB = 7.8, 8 wt% emulsifier, 50/50 wt% aqueous phase/oil phase. Emulsifier system: polyoxyethylene sorbitan trioleate/sorbitan monooleate

(< 200 nm). This allows post-reaction chemical modification, e.g. by the Mannich reaction.

REFERENCES

1. Goin, J., *Water Soluble Polymers*, CEH Marketing Res. Rep. 582.0000 D-E, SRI International, 1991.
2. Minsk, L. M., Kotlarchik, C., Meyer, G. N. and Kenyon, W. O., *J. Polym. Sci., Polym. Chem. Ed.*, 1974, **12**, 133.
3. Vanderhoff, J. W., Bradford, E. B., Tarkowski, H. L., Shaffer, J. B. and Wiley R. M., *Adv. Chem. Ser.*, 1962, **34**, 32.
4. Anon., *Chem. and Eng. News*, 1968, (Jan.), 46.
5. Peaff, G., *Chem. and Eng. News*, 1994, (Nov.), 17.
6. Vanderhoff, J. W., DiStefano, F. V., El-Aasser, M. S., O'Leary, R., Shaffer, O. M. and Visioli, D. L., *J. Disp. Sci. Tech.*, 1984, **5**, 323.
7. Baade, W. and Reichert, K. H., *Eur. Polym. J.*, 1984, **20**, 505.
8. Baade, W. and Reichert, K. H., *Makromol. Chem. Rapid Commun.*, 1986, **7**, 235.
9. Bartelt, G., Ph.D. thesis, Technical University of Berlin, Germany, 1990.
10. Dimonie, M. V., Boghina, G. M., Marinescu, N. N., Cincu, C. J. and Opescu, O. G., *Eur. Polym. J.*, 1982, **18**, 639.
11. Boghina, C. M., Cincu, C. I., Marinescu, N. N., Marinescu, M. M., Dimonie, M. V., Lecca, M., Popescu, G., Oprescu, C. G., Rosanu, A. and Lungu, M., *J. Macromol. Sci.-Chem.*, 1985, **A22**, 591.
12. Pichot, C., Graillat, C., Glukhikh, V. and Lauro, M. F., *Polymer Latex II*, Vol. 11, 1–10. Plastics and Rubber Institute, London.
13. Graillat, C., Pichot, C., Guyot, A., El-Aasser, M. S., *J. Polym. Sci. Polym. Chem. Ed.*, 1986, **24**, 427.
14. Glukhikh, V., Graillat, C. and Pichot, C., *J. Polym. Sci. Polym. Chem. Ed.*, 1987, **25**, 1127.
15. Graillat, C., Lepais-Masmejean, M. and Pichot, C., *J. Disp. Sci. Tech.*, 1990, **11**, 455.
16. Hunkeler, D. J., Hamielec, A. E. and Baade, W., *Polymer*, 1989, **30**, 127.
17. Hunkeler, D. J., *Macromolecules*, 1991, **24**, 2160.
18. Hunkeler, D. J., *Polym. Int.*, 1992, **27**, 23.
19. Hunkeler, D. J., Candau, F., Pichot, C., Hamielec, A. E., Xie, T. Y., Barton, J., Vaskova, V., Guillot, J., Dimonie, M. V. and Reichert, K. H., *Adv. Polym Sci.*, 1994, **112**, 115.
20. Hunkeler, D. J. and Hamielec, A. E., *Polymer*, 1991, **32**, 2626.
21. Candau, F., Leong, Y. S., Pouyet, G. and Candau, F., *J. Colloid Interf. Sci.*, 1984, **101**, 167.
22. Candau, F., Leong, Y. S. and Fitch, R. M., *J. Polym. Sci., Polym. Chem. Ed.*, 1985, **23**, 193.
23. Carver, M. T., Dreyer, U., Knoesel, R., Candau, F. and Fitch, R. M., *J. Polym. Sci., Polym. Chem. Ed.*, 1989, **27**, 2161.
24. Carver, M. T., Candau, F. and Fitch, R. M., *J. Polym. Sci., Polym. Chem. Ed.*, 1989, **27**, 2179.
25. Durand, J. P., Nicholas, N., Kohler, N., Dawans, F. and Candau, F., French Patent No. 2524895, 1984.
26. Kozakiewicz, J. J., Dauplaise, D. L., Schmitt, J. M. and Huang, S. Y., US Patent No. 5037893, 1991.
27. Kozakiewicz, J. J. and Huang, S. Y., US Patent No. 5132023, 1992.
28. Huang, S. Y., Australian Patent No. 650158, 1990.
29. Holtzscherer, C. and Candau, F., *Colloids and Surfaces*, 1988, **29**, 411.
30. Candau, F., Zekhnini, Z., Heatley, F. and Fratna, E., *Colloid and Polym. Sci.*, 1986, **264**, 676.
31. Candau, F., *Encyclopedia of Polymer Science and Technology*, Vol. 9, ed. H. F. Mark, N. M. Bikales, C. G. Overberger and G. Menges. John Wiley, New York, 1987, p. 718.
32. Candau. F., *Polymerization in Organized Media*, ed. C. Paleos. Gordon and Breach, New York, 1992, p. 215.
33. Barton, J. and Capek, I., *Radical Polymerization in Disperse Systems*, VEDA, Publishing House of the Slovak Academy of Sciences, Bratislava, 1991, p. 25.
34. Vaskova, V., Juranicova, V. and Barton, J., *Makromol. Chem.*, 1990, **191**, 717.
35. Vaskova, V., Juranicova, V. and Barton, J., *Makromol. Chem. Macromol. Symp.*, 1990, **31**, 201.
36. Stillhammerova, M. and Barton, J., Paper presented at the 9th International Conference on Modified Polymers, Stara Lesna, Slovakia, 14–18 June, 1993.
37. Barton, J., Tino, J., Hlouskova, Z. and Stillhammerova, M., *Polym. Int.*, 1994, **34**, 89.
38. Hernandez-Barajas, J. and Hunkeler, D. J., *Polym. Mat. Sci. Eng.*, 1993, 69.
39. Candau, F., Leong, Y. S. and Fitch, R. M., *J. Polym. Sci. Polym. Chem. Ed.* 1985, **23**, 193.
40. Hernandez-Barajas, J. and Hunkeler, D. J., *Polym. Adv. Technol.*, 1994, **6**, 509.
41. Hernandez-Barajas, J., Hunkeler, D. J. and Petro, M., *J. Appl. Poly. Sci.*, 1996, **61**, 1325.
42. Hunkeler, D. J., Ni, H., Hernandez-Barajas J. and Petro, M., *Int. J. Polym. Anal. and Charact.*, 1996, **2**, 409.
43. Koehler, K. C., *Physica (Utrecht)*, 1986, **137B**, 320.
44. Wignall, G. D. and Bates, F. S., *J. Appl. Cryst.*, 1986, **20**, 28.
45. Holtzcherer, C., Wittmann, J. C., Guillon, D. and Candau, F., *Polymer* 1990, **31**, 1978.
46. Molyneux, P., *Polym. Mat. Sci. Eng.*, 1987, **57**, 159.
47. Reed, W. and Francois, J., *Macromolecules*, 1991, **24**, 6189.
48. Ying, Q., Wu, G., Chu, B., Farinato, R. and Jackson, J., *Macromolecules*, 1996, **29**, 4646.
49. Hernandez-Barajas, J., Ph.D. thesis, Vanderbilt University, Nashville, TN, 1996.
50. Shinoda, K. and Lindman, B., *Langmuir*, 1987 **3**, 135.
51. Chevalier, Y. and Zemb, T., *Rep. Prog. Phys.*, 1990, **53**, 279.
52. Candau, F., *Scientific Methods for the Study of Polymer Colloids and Their Applications*, ed. F. Candau and R. Ottewill. 1990, Kluewer Academic, Boston, pp. 73–96.
53. Pileni, M. P., *Adv. Colloid Int. Sci.* 1993, **46**, 139.
54. Cabos, C. and Delord, P., *J. Appl. Cryst.*, 1979, **12**, 502.
55. Cabos, C. and Delord, P., *J. Phys. Lett.*, 1980, **41**, 455.
56. Robertus, C., Hoosten, J. G. H. and Levine, Y. K., *Prog. Coll. Polym. Sci.*, 1988, **77**, 115.
57. Brochette, P., Zemb, T., P. Mathis, P. and Pileni, M. P., *J. Phys. Chem.*, 1987, **91**, 1444.
58. Holtzcherer, C., Candau, F. and Ottewill, R., *Prog. Coll. Polym. Sci.*, 1990, **81**, 81.
59. Copart, J. M. and Candau, F., *Macromolecules*, 1993, **26**, 1333.
60. Guinier, A., *Theorie et Technique de la Radiocristallographie*, Dunod, Paris, 1956, p. 329.
61. Higgins, J. S. and Benoit, H. C., *Polymers and Neutron Scattering*. Clarendon Press, Oxford, UK, 1994, p. 141.
62. Kurenkov, V. F., Verzhnikova, A. S. and Myagchenkov, V. A., *Dokl. Akad. Nauk SSR*, 1984, **278**, 1173.
63. Carver, M. T., Dreyer, U., Knoesel, R. and Candau, F., *J. Polym. Sci., Part A: Polym. Chem.*, 1989, **27**, 2161.
64. Hunkeler, D. J. and Hamielec, A. E., *Polymer*, 1991, **32**, 2626.
65. Hunkeler, D. J., Ph.D. thesis, McMaster University, Hamilton, Ont., Canada, 1990.
66. *Azo Polymerization Initiators*, Wako Chemical Industries, 1993.
67. Currie, D. J., Dainton, F. S. and Watt, W. S., *Polymer* 1965, **6**, 451.
68. Ishige, T. and Hamielec, A. E., *J. Appl. Polym. Sci.*, 1973, **17**, 1479.
69. Dainton, F. S. and Tordoff, M., *Trans. Faraday Soc.*, 1953, **53**, 499.
70. Kim, C. J. and Hamielec, A. E., *Polymer*, 1984, **25**, 845.
71. Kulicke, W. M., Kotter, M. and Grujer, M., *Adv. Polym. Sci.*, 1989, **89**, 1.